

*EFFECT OF BATH TEMPERATURE ON THE  
PROPERTIES OF CHEMICALLY DEPOSITED  $\text{Cu}_2\text{O}$  THIN  
FILM*

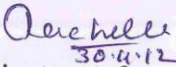
**S.SARASWATHI  
10PHS08**

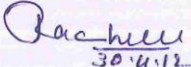
*A thesis submitted to  
Avinashilingam Deemed University For Women, Coimbatore  
in partial fulfilment of the requirements for the  
Master's Degree in Physics  
April, 2012.*

*EFFECT OF BATH TEMPERATURE ON THE  
PROPERTIES OF CHEMICALLY DEPOSITED  $Cu_2O$  THIN  
FILM*

**S.SARASWATHI  
10PHS08**

*A thesis submitted to  
Avinashilingam Deemed University For Women, Coimbatore  
in partial fulfilment of the requirements for the  
Master's Degree in Physics  
April, 2012.*

  
Signature of  
Head of the department

  
Signature of the Supervisor

## ACKNOWLEDGEMENT

*Develop an attitude of gratitude, and give thanks for everything that one achieves knowing that every step forward is a step towards achieving something bigger than your current situation.*

*First and foremost I acknowledge the abundant grace and presence of “Lord Almighty” through the different phases of my project and its successful completion.*

*I extend my deep heartfelt gratitude to **Dr.T.S.K Meenakshisundaram** M.A, M.Phil., Ph.D., Chancellor Avinashilingam Deemed university For Women,Coimbatore, for providing an opportunity to expose myself to the world of knowledge.*

*I express my sincere thanks to **Dr. Sheela Ramachandran**, M.Sc., P.G.Dip., Ph.D, Vice Chancellor, Avinashilingam Deemed university For Women,Coimbatore ,for providing all the administrative support and help required to carry out the project*

*I record my special thanks to **Dr.Gowri Ramakrishnan**, M.Sc., M.Phil., Ph.D., Registrar, Avinashilingam Deemed university For Women,Coimbatore, for the timely help rendered to complete the project successfully.*

*I render my gratitude to **Dr. R.Parvatham**, M.Sc., Dip.Ed, M.phil., Ph.D., Dean, Faculty of science, Avinashilingam Deemed university For Women,Coimbatore, for her valuable support.*

*I express my heartfelt and reverential sense of gratitude to my guide **Dr.Rachel Oommen**, M.Sc.,Dip.Ed. B.Ed,M.phil,Ph.D.,Professor and Head of the Department of Physics, Avinashilingam Deemed university For Women ,Coimbatore, for her constant encouragement, discussion and guidance. Her keen interest and ever-welcoming attitude towards attending to problems paved way for newer ideas and successful completion of my research work.*

*I thank **Ms. Usharajalakshmi** M.Sc., M.Phil., Lecture, Department of physics ,Avinashilingam Deemed university For Women, Coimbatore, for sharing her valuable time, ideas, motivation and for timely suggestions to finish this project.*

*I also express my thanks to Dr. **Thambidurai**, Coimbatore Institute of Technology for his support in characterization studies.*

*I owe my sincere thanks to all the **staff members** of the Department of physics, Avinashilingam Deemed University for Women, Coimbatore, for being supportive and understanding.*

*I am thankful to all **my friends** for their support, understanding and co-operation for the successful completion of the study.*

*No words are sufficient to express my deep sense of gratitude to **my family** for their affection, care and co-operation in all walks of my life.*

**S.SARASWATHI**

<b>TITLE</b>			
<b>LIST OF TABLES</b>			
<b>LIST OF FIGURES</b>			
<b>LIST OF PLATE</b>			
<b>CHAPTER</b>			
<b>1</b>	<b>INTRODUCTION</b>		
	<b>1.1</b>	<b>Deposition technology</b>	
	<b>1.2</b>	<b>Physical deposition</b>	
		<b>1.2.1</b>	<b>Physical Vapor Deposition (PVD)</b>
		<b>1.2.2</b>	<b>Thermal Evaporation</b>
		<b>1.2.3</b>	<b>Electron Beam Evaporation</b>
		<b>1.2.4</b>	<b>Sputter deposition</b>
		<b>1.2.5</b>	<b>Pulsed Laser Deposition</b>
	<b>1.3</b>	<b>Chemical deposition</b>	
		<b>1.3.1</b>	<b>Chemical vapour deposition (CVD)</b>
		<b>1.3.2</b>	<b>Atomic Laser Deposition</b>
		<b>1.3.3</b>	<b>Plasma Enhanced Chemical Vapour Deposition</b>
		<b>1.3.4</b>	<b>Electro Deposition</b>
		<b>1.3.5</b>	<b>Chemical bath deposition(CBD)</b>
	<b>1.4</b>	<b>Cu<sub>2</sub>O Thin Film</b>	
	<b>1.5</b>	<b>Objectives of the study</b>	
<b>2</b>	<b>REVIEW OF LITERATURE</b>		
<b>3</b>	<b>MATERIALS AND METHODS</b>		
	<b>3.1</b>	<b>Successive Ionic Adsorption and Reaction (SILAR)</b>	
		<b>3.1.1</b>	<b>Advantages</b>

		<b>3.1.2</b>	<b><i>Deposition parameters</i></b>
	<b>3.2</b>	<b>Substrate Cleaning</b>	
	<b>3.3</b>	<b>Deposition of the film</b>	
		<b>3.3.1</b>	<b>Chemicals Used</b>
		<b>3.3.2</b>	<b>Preparation Of Solutions</b>
		<b>3.3.3</b>	<b>Film Thickness</b>
	<b>3.4</b>	<b>Characterization</b>	
		<b>3.4.1</b>	<b>X-Ray Diffraction (XRD)</b>
		<b>3.4.2</b>	<b>Scanning Electron Microscopy(SEM)</b>
		<b>3.4.3</b>	<b>UV-Visible Spectroscopy</b>
<b>4</b>	<b>RESULTS AND DISCUSSION</b>		
	<b>4.1</b>	<b>Structural properties</b>	
	<b>4.2</b>	<b>Scanning Electron Microscopy (Morphology)</b>	
	<b>4.3</b>	<b>Optical properties</b>	
<b>5</b>	<b>SUMMARY AND CONCLUSION</b>		
	<b>REFERENCE</b>		

## LIST OF FIGURES

FIGURE NUMBER	CAPTION
3.1	Schematic diagram of X-ray diffraction
3.2	Schematic diagram of Scanning Electron Microscope
3.3	Schematic diagram of the UV-Visible spectrometer
4.1	XRD pattern of as-prepared copper oxide thin film sample 1
4.2	XRD pattern of as-prepared copper oxide thin film sample 2
4.3	XRD pattern of as-prepared copper oxide thin film sample 3
4.4	XRD pattern of annealed (200°C) copper oxide thin film sample 1
4.5	XRD pattern of annealed (200°C) copper oxide thin film sample 2
4.6	XRD pattern of annealed(200°C) copper oxide thin film sample 3
4.7	XRD pattern of annealed(250°C) copper oxide thin film sample 1
4.8	XRD pattern of annealed (250°C) copper oxide thin film sample 2
4.9	XRD pattern of annealed (250°C) copper oxide thin film sample 3
4.10	Scanning Electron Micrograph of Cu <sub>2</sub> O film deposited on glass substrate.
4.11	Optical transmittance (T) Spectra of as-prepared and annealed thin copper oxide film Sample 1
4.12	Optical transmittance (T) Spectra of as-prepared and annealed thin copper oxide film Sample 2
4.13	Optical transmittance (T) Spectra of as-prepared and annealed thin copper oxide film Sample 3
4.14	Absorption Spectra of as-prepared and annealed thin copper oxide film Sample 1
4.15	Absorption Spectra of as-prepared and annealed thin copper oxide film Sample 2
4.16	Absorption Spectra of as-prepared and annealed thin copper oxide film Sample 3

4.17	$(\alpha h\nu)^2$ Vs $h\nu$ Plot of as-deposited Sample 1
4.18	$(\alpha h\nu)^2$ Vs $h\nu$ Plot of annealed (200°C) Sample 1
4.19	$(\alpha h\nu)^2$ Vs $h\nu$ Plot of annealed (250°C) Sample 1
4.20	$(\alpha h\nu)^2$ Vs $h\nu$ Plot of as- deposited Sample 2
4.21	$(\alpha h\nu)^2$ Vs $h\nu$ Plot of annealed (200°C) Sample 2
4.22	$(\alpha h\nu)^2$ Vs $h\nu$ Plot of annealed (250°C) Sample 2
4.23	$(\alpha h\nu)^2$ Vs $h\nu$ Plot of as-deposited Sample 3
4.24	$(\alpha h\nu)^2$ Vs $h\nu$ Plot of annealed (200°C) Sample 3
4.25	$(\alpha h\nu)^2$ Vs $h\nu$ Plot of annealed (250°C) Sample 3
4.26	variation of transmittance with wave length of Cu <sub>2</sub> O thin film
4.27	variation of absorption with wave length of Cu <sub>2</sub> O thin film
4.28	variation of Band gap with temperature of the precursor solution of Cu <sub>2</sub> O thin film
4.29	variation of grain size with temperature of the precursor solution of Cu <sub>2</sub> O thin film
4.30	variation of thickness with temperature of the precursor solution of Cu <sub>2</sub> O thin film

## LIST OF PLATES

<b>PLATE NUMBER</b>	<b>TITLE</b>
I	Experimental set up of SILAR Deposition Method

# CHAPTER-1

## INTRODUCTION

“A thin film is a layer of material ranging from the fraction of a nanometer to several micro meters in thickness”. Thin film is the branch of optics that deals with very thin structured layer of different materials. A microscopically thin layer of material that is deposited on to a metal, ceramic semiconductor, insulator or dielectrics etc....Typically less than one micron thick. Thin film can be conductive (or) dielectric (non conductive) and are used in myriad application. It may be arbitrarily defined as a solid layer having a thickness varying from a few Ångströms to micrometers.

In order to produce such thin films, the deposit must be applied in a very controlled manner, sometimes even atomic monolayer, under extremely clean, particulate free conditions. Individual depositing particles must be able to travel from some deposition source to the substrate to be coated with little or no collision with gas molecules on the way (a long 'mean free path') - thin film deposition is a high vacuum process.

### 1.1 Deposition technology

Thin film deposition is a process in which the physical characteristics of a surface are modified by applying a very thin coating, often just a few millionths of a millimeter thick. Thin films can be used to modify the optical characteristics of a surface (the substrate), its electrical conductivity, its hardness or lubricity, to provide corrosion resistance or chemical inertness, or simply for decoration. Every-day examples of thin films include the reflective coating on CDs and DVDs, anti-reflective coatings on spectacles and thermally efficient double glazing (optical films), the tiny electrical pathways within a micro-processor (electrical films), hardened machine tool bits (hardness), to food and drug packaging (decoration and passivation).

Techniques involved are physical vapour deposition, thermal deposition, sputtering, electron beam evaporation etc. and chemical vapour deposition, plasma enhanced chemical vapor deposition, atomic laser deposition and chemical deposition, chemical bath deposition.

## 1.2 Physical deposition

### 1.2.1 Physical Vapour Deposition

Physical vapour deposition uses mechanical or thermodynamic means to produce the thin film. The principal mechanical method is a technique known as sputtering, where energetic noble gas ions, most commonly Argon, bombard the surface of a target made from the desired film material, releasing a plume of material from the target - like the shower of earth produced when a shell hits the ground - which then embeds itself into the surface of the substrate. Thermal evaporation (thermodynamic means) is a process in which a solid piece of the desired film material is heated until it melts and then evaporates or until it sublimates. Under high vacuum the vapour follows a direct line of sight path to the substrate where it condenses to form the thin film. Materials can be deposited with improved properties compared to the substrate material. Almost any type of inorganic material can be used as well as some kinds of organic materials. The process is more environmentally friendly than processes such as electroplating.

### 1.2.2 Thermal Evaporation

One of the common methods of Physical Vapor Deposition (PVD) is Thermal Evaporation. This is a form of Thin Film Deposition, which is a vacuum technology for applying coatings of pure materials to the surface of various objects. Thermal Evaporation involves heating a solid material inside a high vacuum chamber, taking it to a temperature which produces some vapor pressure. Inside the vacuum, even a relatively low vapor pressure is sufficient to raise a vapor cloud inside the chamber. This evaporated material now constitutes a vapor stream, which traverses the chamber and hits the substrate, sticking to it as a coating or film. Most Thermal (Filament or E Beam) Evaporation PVD systems include quartz crystal deposition control, whereby real time deposition rate monitoring and control takes most of the work out of achieving the right thickness thin Film Evaporation systems can also be configured with various hardware or software options. These can include ion source capability either for in situ cleaning of substrate surfaces or for ion assisted deposition, or substrate pre heat stations. Other options can include multiple quartz crystals, co-deposition with multiple sources (either type), or fast cycle load lock stations.

### 1.2.3 Electron beam Evaporation

Electron beam evaporation is the most versatile means of vacuum evaporation and deposition. This technique allows the production of thin film coatings from pure elements, including most metals, as well as numerous alloys and compounds. Electron beam evaporation offers several advantages over competing processes including precise control of low or high deposition rates, excellent material utilization, co-deposition and sequential deposition systems and a uniform low temperature deposition. Electron beam offers higher evaporation rates, freedom from contamination and precise rate control at very low deposition levels, precise film composition and cooler substrate temperatures. The materials used for evaporation are available in near limitless shapes and forms, the most common being pellet slugs and disks. Electron beam evaporation is an extremely versatile means of depositing uniform high-purity thin films. Capable of reaching elevated temperatures in excess of 3500°C, evaporation of virtually any material can be accomplished.

### 1.2.4 Sputter Deposition

When an energetic particle strikes a surface (the target), a plume of material is released, like the shower of sand when a golf ball lands in the bunker. This effect is known as 'sputtering' and is used to produce films of materials as thin as just a few millionths of a millimeter. The source of the ions might either be local plasma (diode or planar magnetron sputtering) or a separate ion beam source (ion beam deposition).

### 1.2.5 Pulsed laser Deposition

The technique of Pulsed laser deposition has been used to deposit high quality films of materials for more than a decade. The technique uses high power laser pulses (typically  $\sim 10^8 \text{ Wcm}^{-2}$ ) to melt, evaporate and ionize material from the surface of a target.

## 1.3 Chemical Deposition

The deposition of film from aqueous solutions either by passing a current or by chemical reactions under appropriate conditions and is generally used for the deposition of thick metallic or alloy film. Despite limitation this technique is widely used for the fabrication of conducting connectors, magnetic memory elements, etc.

with an appropriate control the deposition parameters such as bath composition, temperature, PH, etc...

### 1.3.1 Chemical Vapour Deposition

Thin film deposition processes broadly fall into chemical vapour deposition (CVD). In CVD the substrate is exposed to one or more volatile precursors, which react and/or decompose on the substrate surface to produce the desired deposit. Frequently, volatile by products are also produced, which are removed by gas flow through the reaction chamber. The growth of the film is often enhanced either by heating the substrate, or by using plasma to increase the density of reactive species (free radicals). In some cases both are used, such as in the deposition of diamond like carbon (DLC) where carbon is deposited at high temperatures (typically in excess of 800<sup>0</sup>c).

The utility of chemical vapour deposition to grown thin film is widely recognized in the semiconductor industry. The cvd process provides thin film with a high uniformity in a chemical composition. The ability to cover any geometric shape with a deposit of crystalline nano particles.

### 1.3.2 Atomic layer Deposition

Atomic layer deposition offers precise control of depositions down to the atomic scale. From accelerating the speed of semiconductors to improving the efficiency of solar panels. ALD holds tremendous promise across a wide array of industries, including energy, optical, electronics, nanostructures, biomedical, and more. The **principle of ALD** is based on sequential pulsing of special precursor vapors, each of which forms about one atomic layer each pulse.

### 1.3.3 Plasma Enhanced Chemical Vapour Deposition

Plasma Enhanced Chemical Vapour Deposition causes the reactive gases to decompose via the electrical discharge. This causes films to deposit at lower temperatures than CVD. The properties of microelectronic circuits deposited via PECVD can thus be improved over CVD.

### 1.3.4 Electrodeposition

Electro deposition is also known as "electroplating" and is typically restricted to electrically conductive materials. There are basically two technologies for plating: Electroplating and Electro less plating. In electroplating process the substrate is placed in a liquid solution (electrolyte). When an electrical potential is applied between a conducting area on the substrate and a counter electrode (usually platinum) in the liquid, a chemical redox process takes place resulting in the formation of a layer of material on the substrate and usually some gas generation at the counter electrode.

Electro less deposition is the process of depositing a coating with the aid of a chemical **reducing agent** in solution, and without the application of external **electrical power**. It is therefore applicable to **non-conducting** substrates, and has been used extensively for metallizing printed wiring boards (PWB). Though electro less metal deposition rates are typically lower than those of electrolytic deposition rates, as dimensions of circuit lines continue to get smaller, electro less deposition will continue to be attractive for next generation PWB products which have much finer and thinner lines than traditional PWB products. More recently, selective electro less deposition has been found to yield encouraging results in the case of the self-aligned cobalt-tungsten-phosphorus alloy capping, or barrier, layer on back-end-of-line (BEOL) copper interconnects, for example, in tests aimed at high performance logic chips at the CMOS 45 **nm** node and below.

### 1.3.5 Chemical Bath Deposition

The Chemical bath deposition (CBD) method is one of the cheapest methods to deposit **thin films** and **nanomaterials**, as it does not depend on expensive equipment and is a scalable technique that can be employed for large area batch processing or continuous deposition. In 1933 Bruckman deposited **Lead (II) sulfide** (PbS) thin film by chemical bath deposition (CBD) or solution grown method. The major advantage of CBD is that it requires only solution containers and substrate

mounting devices. The Chemical Bath deposition (CBD) is an electroless technique that is attractive as a simple and low cost method (Ramaiah, 2001). The method is well studied and produces films that have comparable structural and optoelectronic properties to those produced using other sophisticated thin film deposition techniques (Chanda et al., 1980). The technique has been applied in producing materials for solar cells, protective coating, thermal controls in buildings and is being adopted by some industries (Osuji, 2003).

Among various deposition techniques, chemical bath deposition yields stable, adherent, uniform and hard films with good reproducibility by a relatively simple process. The chemical bath deposition method is one of the suitable methods for preparing highly efficient thin films in a simple manner. The growth of thin films strongly depends on growth conditions, such as duration of deposition, composition and temperature of the solution, and topographical and chemical nature of the substrate.

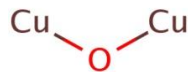
Chemical bath deposition (CBD) is a convenient and low cost technique for growing thin films of many types of materials. Chemical Solution Deposition (CSD) comprise all solution based thin film deposition techniques which involve chemical reactions of precursors during the formation of the oxide films, i.e. sol-gel type routes, metallo-organic decomposition routes, hybrid routes, etc. CSD has emerged as a highly flexible and cost-effective technique for the fabrication of a very wide variety of functional oxide thin films. Application areas include, for example, integrated dielectric capacitors, ferroelectric random access memories, pyroelectric infrared detectors, piezoelectric micro-electromechanical systems, antireflective coatings, optical filters, conducting-, transparent conducting-, and superconducting layers, luminescent coatings, gas sensors, thin film solid-oxide fuel cells.

## 1.4 Cuprous Oxide

$\text{Cu}_2\text{O}$  Crystals with different shapes consist of different atomic arrangements on the surface (e.g. surface termination, symmetry, inter atomic distances) which directly affect a material's reactivity and stability. Therefore, the ability to systematically tune the shape of a material would be invaluable in adjusting its properties and elucidating shape-property relationships. Cuprous oxide ( $\text{Cu}_2\text{O}$ ) is an

oxide of copper also known as Copper (I) oxide. It is insoluble in water and organic solvents. Cuprous oxide is commonly used as a pigment, a fungicide and an antifouling agent for marine paints.

Crystal habit can be regulated by introducing additives that preferentially adsorb onto specific crystallographic planes. While crystal habit mainly depends on the composition of the plating solution, the degree of branching can be independently regulated by controlling the reaction rate or over potential. The chemical formula for cuprous oxide is  $\text{Cu}_2\text{O}$ . This inorganic compound is used as a fungicide and as a red coloring pigment for glass and ceramic glazes. Cuprous oxide is also used in marine paints as an antifouling product.



$\text{Cu}_2\text{O}$  thin film have been prepared by various techniques like chemical vapour deposition, anodic deposition, thermal oxidation, spray pyrolysis, sol-gel method, electro deposition, chemical vapor deposition, etc... The air annealed copper films were characterized for their structural, electrical and optical properties by using X ray diffraction, scanning electron microscope, electrical resistivity and optical measurement technique.  $\text{Cu}_2\text{O}$  is still attractive cheaper for the advantages of high absorption coefficient in the visible region, non toxicity, abundant availability and low- cost producibility. The  $\text{Cu}_2\text{O}$  films obtained by the high chemical purity and their thickness can be easily controlled during the deposition process.  $\text{Cu}_2\text{O}$  thin film was deposited in glass substrate by modified chemical bath deposition.

### 1.5 Objectives of the study

The aim of the present work is

- ❖ To prepare  $\text{Cu}_2\text{O}$  thin film by chemical bath deposition technique on glass substrate.
- ❖ To study the effect of precursor solution temperature on the structural and optical properties of the film.

- ❖ To analyze structural and optical properties of the coated thin film using UV/visible, X ray diffractometer, Scanning electron microscope characterization methods.

## CHAPTER-2

### REVIEW OF LITERATURE

Well-defined polycrystalline  $\text{Cu}_2\text{O}$  was electrodeposited on transparent conducting substrates from alkaline  $\text{Cu(II)}$  lactate solutions by De Jongh P. E., et al.,(1999).The morphology of the layers could be controlled by choosing the appropriate experimental conditions; the pH and temperature of the deposition solution were especially important. The growth of the oxide involves a thermally activated process, for which an activation energy of 0.8 eV was found. A mechanism for the deposition is proposed. The optical absorption of the electrodeposited oxide in the visible range was much weaker than expected for a direct semiconductor with a band gap of 2.0 eV. Finally, it was also shown that it is possible to grow  $\text{Cu}_2\text{O}$  inside an n-type  $\text{TiO}_2$  nanoporous matrix.

Electrochemical deposition of cuprous oxide ( $\text{Cu}_2\text{O}$ ) thin films on tin-oxide-coated glass and copper substrates by cathodic reduction of alkaline cupric lactate solution has been investigated by Mahalingam T. et al.,( 2000) between  $60^\circ\text{C}$  and  $80^\circ\text{C}$ . Deposition kinetics of cuprous oxide thin films were studied and the parameters limit for the deposition of the films were determined. Structure of the deposited film is simple cubic with a preferential orientation of (2 0 0). Optical absorption studies reveal 1.99 eV for band gap and optical constants ( $n,k$ ) are evaluated. Electrical resistivity studies are carried out in the temperature range  $27^\circ\text{C}$ – $330^\circ\text{C}$ .

The electrodeposition of cuprous oxide ( $\text{Cu}_2\text{O}$ , red copper oxide) on Pt cathode in a weak acidic electrolyte was executed by the current modulation method by Jaeyoung Lee et al.,(2000).The formation mechanism of  $\text{Cu}_2\text{O}$  was investigated by electrochemical characteristics analysis utilizing electrochemical quartz crystal microbalance (EQCM), chronopotentiometry (CP), and pulsed current methods. A scanning electron microscope and X-ray diffractometer were also used for investigation of the mechanism for  $\text{Cu}_2\text{O}$  film growth. EQCM and CP results indicate that the dissolution potentials of Cu and  $\text{Cu}_2\text{O}$  were different and were used for the selective dissolution of copper when the pulsed anodic current was applied. Pulsed electrodeposition technique offered a useful method in preparing  $\text{Cu}_2\text{O}$  thin film, in

which both Cu metal and Cu<sub>2</sub>O phases were electrodeposited on platinum electrode, when a higher cathodic current, -5.0 mA/cm<sup>2</sup>, was constantly applied in a 10 mM copper nitrate solution. The cycling of current led to the rapid formation of a single phase of Cu<sub>2</sub>O thin film, which was uniform and compact.

Georgieva .V, Ristov.M (2001). prepared Semiconducting cuprous oxide films by electrodeposition onto commercial conducting glass coated with indium tin oxide deposited by spraying technique. The cuprous oxide (Cu<sub>2</sub>O) films were deposited using a galvanostatic method from an alkaline CuSO<sub>4</sub>bath containing lactic acid and sodium hydroxide at a temperature of 60<sup>0</sup> C. The film's thickness was about 4–6 μm. This paper includes discussion for Cu<sub>2</sub>O films fabrication, scanning electron microscopy and X-ray diffractometry studies, optical properties and experimental results of solar cells. The values of the open circuit voltage Voc of 340mV and the short circuit current density Isc of 245 mA/cm<sup>2</sup> for ITO/Cu<sub>2</sub>O solar cell were obtained by depositing graphite paste on the rear of the Cu<sub>2</sub>O layer. It should be stressed that these cells exhibited photovoltaic properties after heat treatment of the films for 3h at 130<sup>0</sup>C. An electrodeposited layer of Cu<sub>2</sub>O offers wider possibilities for application and production of low cost cells, both in metal–semiconductor and hetero-junction cell structures, hence the need to improve the photovoltaic properties of the cells.

Mukhopadhyay A.K. et al.,(2001) Semiconducting cuprous oxide (Cu<sub>2</sub>O) thin films, important for low cost solar cell and oxygen or humidity sensor applications, were galvanostatically deposited at 40–60 °C on copper substrates. The deposition kinetics, studied up to a film thickness of about 20 μm, was found to be linear and independent of deposition temperature. The observed film growth rate was in excellent agreement with the growth rates predicted from Faraday's law of electrolysis. The deposited films exhibited a preferred (200) orientation. The current-voltage characteristics of the electrodeposited Cu<sub>2</sub>O/Cu diodes exhibited a metal-insulator-semiconductor type of behaviour, suggesting the presence of a thin interfacial insulating layer between Cu<sub>2</sub>O and copper. The electrical conductivity of Cu<sub>2</sub>O films was found to vary exponentially with temperature in the 145–300°C range with an associated activation energy of 0.79 eV.

Sekhar C. (2001) Prepared copper oxide films using a methanolic solution of cupric chloride (CuCl<sub>2</sub> · 2H<sub>2</sub>O) by the sol–gel-like dip technique at different baking

temperatures. XRD study confirms that the films are of  $\text{Cu}_2\text{O}$  phase when prepared at a baking temperature of  $360^\circ\text{C}$  and  $\text{CuO}$  phase when prepared at  $400\text{--}500^\circ\text{C}$  baking temperature. The optical direct band gap energies for  $\text{Cu}_2\text{O}$  and  $\text{CuO}$  films calculated from optical absorption measurements are 2.10 and 1.90 eV, respectively, which are quite comparable with the reported values.

Jorge Medina-Valtierra et al.,(2002)  $\text{Cu}_2\text{O}$ – $\text{CuO}$  and  $\text{CuO}$  thin films on a fiberglass substrate were prepared by chemical vapor deposition (CVD) and then catalytically evaluated by cyclohexane oxidation. The fiber with a  $\text{Cu}_2\text{O}$ – $\text{CuO}$  film showed a high catalytic activity at low temperatures, for example 43% at  $350^\circ\text{C}$ , and a good selectivity to cyclohexanol production (37% at  $300^\circ\text{C}$ ). The fiber with a  $\text{CuO}$  film exhibited a higher catalytic activity, for example 48% at  $350^\circ\text{C}$ , with a high yield of cyclohexanone (37% at  $250^\circ\text{C}$ ). A  $\text{CuO}/\text{SiO}_2$  catalyst with the same  $\text{CuO}$  content gave a result similar to the  $\text{CuO}/\text{fiberglass}$  system under the same conditions examined but, on the other hand cyclohexane was cleaved giving a higher selectivity to hexenes, 30% at  $250^\circ\text{C}$ . The effect of reaction temperature on the catalytic activity and selectivity of cyclohexane oxidation were investigated. At  $300^\circ\text{C}$  the steady-state catalytic performance of the  $\text{CuO}/\text{fiberglass}$  experienced a slight deactivation after 4 h time-on stream from 40% to 38% of conversion , after which the catalyst could be reused apparently without any activity loss.

Mahalingam T.et al., (2002) Semiconducting  $\text{Cu}_2\text{O}$  thin films were electrodeposited potentiostatically on  $\text{Cu}$  and  $\text{SnO}_2$  substrates. The deposition kinetics of film growth and the conditions to obtain spotty and uniform  $\text{Cu}_2\text{O}$  films are studied. X-ray diffraction studies revealed the formation of single phase cubic  $\text{Cu}_2\text{O}$  films. The effects of deposition potential, solution pH and bath temperature on the structure are studied. The optical, electrical, composition and morphological analysis are carried out for  $\text{Cu}_2\text{O}$  films prepared at various deposition conditions.

Ristov M. et al.,(2002) Described a simple method for the chemical deposition of  $\text{Cu}_2\text{O}$  thin films. The films obtained by this method are of high chemical purity and their thicknesses can easily be controlled during the deposition process. The physical properties of the films were examined and compared with the properties of  $\text{Cu}_2\text{O}$  obtained by other methods.

Chatterjee A.P. et al.,(2003) Prepared Semiconducting cuprous oxide films by electrodeposition onto copper substrates from an alkaline  $\text{CuSO}_4$  bath at temperatures between 40 and 60°C. The  $\text{Cu}_2\text{O}$  films, which were deposited using a potentiostatic method, were found to exhibit exponential growth kinetics. X-ray diffraction studies revealed the formation of only  $\text{Cu}_2\text{O}$  films with (200) preferred orientation. The observed current-voltage characteristics of the device structures were found to be similar to that of a metal-insulator-semiconductor (MIS) tunnel diode, indicating the presence of a thin unidentified interfacial insulating layer between the copper substrate and the cuprous oxide film.

**Mahalingam T. et al.,(2003)** Synthesised Cuprous oxide ( $\text{Cu}_2\text{O}$ ) thin films on Cu and tin oxide coated substrates by electrochemical pulse plating technique. The effect of current density and duty cycle on the growth of  $\text{Cu}_2\text{O}$  films is studied. Structural studies reveal an optimum duty cycle of 33% to deposit well-crystallized  $\text{Cu}_2\text{O}$  film. The effect of deposition parameters on the structural and optical properties are carried out. It is observed that annealing below 350°C improved the crystallinity and grain size of  $\text{Cu}_2\text{O}$  films whereas annealing above 450°C exhibited the conversion of  $\text{Cu}_2\text{O}$  into  $\text{CuO}$ . Photoelectrochemical solar cell studies showed improved performance for  $\text{Cu}_2\text{O}$  electrodes and the results are discussed.

Ivan Grozdanov (2003) Developed an electroless, solution growth deposition technique for  $\text{Cu}_2\text{O}$  thin films, suitable for large-area depositions at relatively low temperatures (70°C). Uniform and electro conductive  $\text{Cu}_2\text{O}$  films were deposited on glass or clear polyester film substrates, pre-coated with an ultrathin layer of  $\text{Cu}_x\text{S}$ . Post-deposition treatment of the chemically deposited  $\text{Cu}_2\text{O}$  films in diluted solutions of  $\text{Na}_2\text{S}$  resulted in further increase of conductivity and absorbance. Rutherford backscattering analyses confirmed sulfur implantation into the  $\text{Cu}_2\text{O}$  films.

Cuprous oxide ( $\text{Cu}_2\text{O}$ ) thin films were deposited on Cu and tin oxide coated glass substrates through potentiostatic electrodeposition by Mahalingam T. et al.,(2005). the optimum range of deposition parameters was experimentally investigated. X-ray diffraction studies revealed the formation of single-phase cubic  $\text{Cu}_2\text{O}$  films in the deposition potential range from -0.355 to -0.555V versus SCE. Studies revealed that an optimum pH of 9.0 yielded single-phase cubic films with

improved crystallinity. The preferential orientation of (2 0 0) cubic Cu<sub>2</sub>O peak was found to increase with bath temperature in the range 30–70°C. The effects of annealing on the preferred orientation, grain size and optical band gap were studied. The energy conversion efficiencies of as-deposited and annealed p- Cu<sub>2</sub>O films as photocathodes in photoelectrochemical (PEC) solar cells were studied and the results were discussed.

Akimoto K. et al.,(2005) Studied deposition conditions of cuprous oxide (Cu<sub>2</sub>O) thin films on glass substrates and nitrogen doping into Cu<sub>2</sub>O by using reactive radio-frequency magnetron sputtering method. The effects of defect passivation by crown-ether cyanide treatment, which simply involves immersion in KCN solutions containing 18-crown-6 followed by rinse, were also studied. By the crown-ether cyanide treatment, the luminescence intensity due to the near-band-edge emission of Cu<sub>2</sub>O at around 680 nm was enhanced, and the hole density was increased from 10<sup>16</sup> to 10<sup>17</sup> cm<sup>-3</sup>. Finally, polycrystalline p-Cu<sub>2</sub>O/n-ZnO heterojunctions were grown for use in solar cells. Two deposition sequences were studied, ZnO deposited on Cu<sub>2</sub>O and Cu<sub>2</sub>O deposited on ZnO. It was found that the crystallographic orientation and current–voltage characteristics of the heterojunction were significantly influenced by the deposition sequence, both being far superior for the heterojunction with structure Cu<sub>2</sub>O on ZnO than for the inverse structure.

Yueh-Hsun Lee et al.,(2006) The (2 0 0) and (1 1 1) preferred Cu<sub>2</sub>O thin films are prepared by electrochemical deposition from copper-lactate system. The texture of the films could be modified by simply changing the bath pH or overpotential. The detailed microstructure and its evolution are also observed by both scanning electron microscopy and transmission electron microscopy. It is found that the growth of the (2 0 0) preferred films is achieved by the columnar growth with a coalescence mechanism, but that of the (1 1 1) preferred films is the growth involving a secondary nucleation and growth. It is also found that the (2 0 0) textured films exhibit better electrochemical property toward Li than the (1 1 1) textured ones due to the different microstructure features originating from different growth behavior.

Xun Li, Feifei Tao et al.,(2007) Cuprous oxide 3-D ordered macroporous material was constructed by electrochemical deposition using a polystyrene colloidal crystal as template. The highly ordered macroporous structure with a hexagonal array can be extended over hundreds of square micrometers. The photonic stop bands of both the PS colloidal crystal and Cu<sub>2</sub>O 3DOM were found. Due to the highly ordered

porous structure, the optical absorption and the charge carrier transportation are better in Cu<sub>2</sub>O 3DOM than in bulk Cu<sub>2</sub>O, which makes the reduction of oxygen faster on Cu<sub>2</sub>O 3DOM than on bulk Cu<sub>2</sub>O under visible light illumination. The higher photocurrent efficiency under visible light illumination makes the 3DOM Cu<sub>2</sub>O more suitable for solar applications.

Neskovska.R et al.,(2007) prepared thin cuprous oxide films by a low cost, chemical deposition (electroless) method onto glass substrates pre-coated with fluorine doped tin oxide. The X-ray diffraction pattern confirmed the Cu<sub>2</sub>O composition of the films. Visible transmittance spectra of the cuprous oxide films were studied for the as-prepared, colored and bleached films. The cyclic voltammetry study showed that those films exhibited cathode coloring electrochromism, i.e. the films showed change of color from yellowish to black upon application of an electric field. The transmittance across the films for laser light of 670 nm was found to change due to the voltage change for about 50%. The coloration memory of those films was also studied during 6 h, ex-situ. The coloration efficiency at 670 nm was calculated to be 37 cm<sup>2</sup>/C.

Cuprous oxide (Cu<sub>2</sub>O) thin films were grown by SeongHo Jeong et al.,(2009) epitaxially on c-axis-oriented polycrystalline zinc oxide (ZnO) thin films by low-pressure metal organic chemical vapor deposition (MOCVD) from Copper(II) hexafluoroacetylacetonate at various substrate temperatures, between 250 and 400<sup>0</sup>C, and pressures, between 0.6 and 2.1 Torr. Polycrystalline thin films of Cu<sub>2</sub>O grow as single phase with 110 axis aligned perpendicular to the ZnO surface and with in-plane rotational alignment due to epitaxy. The resulting interface is rectifying and may be suitable for oxide-based pn junction solar cells or diodes.

Long-cheng wang et al.,(2009) **Micro-crystals of cuprous oxide with different morphologies were prepared by a hydrothermal process with copper sulfate and sodium lactate as precursors. Morphology of cuprous oxide was simply controlled by adjusting solution pH values or addition of different amounts of organic solvent. Structural properties of all the samples were characterized by X-ray diffraction and scanning electron microscopy. The growth mechanism of cuprous oxide micro-crystal under different conditions was discussed. Results show that morphologies of cuprous oxide micro-crystals**

**alter from branched structure to octahedron structure and cube structure with growth conditions.**

Cu<sub>2</sub>O thin films were deposited by SEONGHO JEONG ET AL.,(2010) on ZnO coated glass substrates by metal organic chemical vapor deposition from copper(II) hexafluoroacetylacetonate [Cu(C<sub>5</sub>HF<sub>6</sub>O<sub>2</sub>)<sub>2</sub>], oxygen gas, and water vapor. The dependence of the structural and electrical properties of Cu<sub>2</sub>O films on deposition temperature and film thickness was investigated. X-ray diffraction showed that Cu<sub>2</sub>O thin films grow on ZnO with preferred (220)<sub>Cu<sub>2</sub>O</sub> || (0002)<sub>ZnO</sub> orientation. The grain size and stress in Cu<sub>2</sub>O films increase with increasing substrate temperature but decrease with increasing film thickness. The carrier mobility increases with increasing grain size indicating that the carrier transport is limited by scattering from the grain boundaries. Single-phase epitaxial p-type Cu<sub>2</sub>O films with hole mobilities exceeding cm<sup>2</sup>/V s are obtained at a deposition temperature of 400 °C.

Muhammad muhibbullah et al.,(2010) Deposited copper oxide thin films by the chemical bath deposition technique. CuSO<sub>4</sub> and Na<sub>2</sub>SO<sub>3</sub> were used to prepare the deposition solution, and the solution was heated to 70–80 °C. The deposited films are crystalline with a cubic crystal structure and have Cu/O ratios of 1.7–1.8. The oxygen content can be increased by bubbling oxygen gas into the solution during the deposition. It was confirmed by photo-electrochemical measurement that the films are p-type and photoconductive. Thus, the films are potentially useful for photovoltaic applications.

Lila Chaal et al.,(2010) The normal and lateral spring constants of rectangular silicon AFM cantilevers bearing pyramidal silicon tips were accurately calibrated using a procedure that takes into account their tilt compared to horizontal orientation and their trapezoidal cross section. Such systems were used to carry out nanoscratching tests in air on technical substrates presenting a moderate roughness (RMS ≈ 40 nm) and made either from bulk copper or from cuprous oxide thin films electrogenerated on copper. The various events occurring during these nanoscratching procedures were characterized in details. In particular, the features of the scars appearing on the scratched zones and SEM observations of the AFM tips used during the nanoscratching procedures are described and exploited to establish a better understanding of the effects of the nanoscratching procedures on the targeted samples. In the case of electrodeposited Cu<sub>2</sub>O films, these effects are discussed with the help of chemical and structural characterizations using XPS and XRD studies. All this set of

information is used i) to describe the history of the nanoscratching tests and ii) to compare mechanical resistance of bulk copper and electrogenerated  $\text{Cu}_2\text{O}$  thin films using these nanoscratching tests carried out in air.

Prakash Bansilal Ahirrao et al.,(2010) Cuprous oxide ( $\text{Cu}_2\text{O}$ ) is an interesting p-type semiconductor material used in solar cell applications. The Modified chemical bath deposition (M-CBD) method is suitable for growing thin multilayer structure due to low deposition temperature. This method does not require any sophisticated instrument and substrate need not to be conductive. The nanocrystalline  $\text{Cu}_2\text{O}$  thin films were deposited on glass substrates by M-CBD method. The deposited films were characterized by different characterization techniques to study structural, surface morphological, optical and electrical properties. The structural studies show that, the formation of  $\text{Cu}_2\text{O}$  thin films with an average crystallite size of 14 nm. Optical studies show a direct band gap 2.48 eV. The room temperature electrical resistivity is of the order of  $1.3 \text{ kW cm}$  and activation energy 0.33 eV. The films exhibit p-type electrical conductivity as seen by thermo-emf measurements.

Xiao Jiao Yu et al.,(2011) Prepared  $\text{Cu}_2\text{O}$  thin films through electrodeposition with conductive glass of coating indium tin oxide as work electrode. The effects of various factor upon  $\text{Cu}_2\text{O}$  film morphology are investigated. The best conditions of electrodeposition  $\text{Cu}_2\text{O}$  film are discussed. The deposition potential is determined by Linear sweep voltammetry. The results indicate that when pH is 5.50~ 6.00, the concentrations of  $\text{Cu}(\text{CH}_3\text{COO})_2$  is 0.015 ~ 0.04 mol/L, and the deposition potential is -0.075 ~ -0.225 V (vs SCE),  $\text{Cu}_2\text{O}$  thin films morphology is dendritic crystal.

**CLAUDIA MALERBA ET AL.,(2011)** The optical absorption coefficient of thin film and bulk  $\text{Cu}_2\text{O}$  at room temperature is obtained from an accurate analysis of their transmittance and reflectance spectra. These absorption spectra are modeled, together with the low temperature data reported in the literature, using an analytical expression to assess and quantify the role of the different absorption mechanisms. The results suggest that direct forbidden transitions and indirect transitions play an almost equally relevant role.

Balasubramaniam K. R. et al.,(2012) The proof-of-concept of using an abundantly occurring natural ore, malachite ( $\text{Cu}_2\text{CO}_3(\text{OH})_2$ ) to directly yield the semiconductor  $\text{Cu}_2\text{O}$  to be used as an active component of a functional thin film based

device.  $\text{Cu}_2\text{O}$  is an archetype hole-conducting semiconductor that possesses several interesting characteristics particularly useful for solar cell applications, including low cost, non-toxicity, good hole mobility, large minority carrier diffusion length, and a direct energy gap ideal for efficient absorption. The structural, optical, and electrical transport characteristics of  $\text{Cu}_2\text{O}$  thin films grown from the natural mineral malachite and synthetic  $\text{CuO}$  targets.

## **CHAPTER-3**

### **MATERIALS AND METHODS**

Successive Ionic Layer Adsorption and Reaction (SILAR) method has been used to deposit Cu<sub>2</sub>O thin film. The SILAR method is a modified chemical bath deposition (CBD) method. The preparative conditions such as concentration, pH, temperature of the precursors, immersion time, immersion cycles, etc. are optimized to get Cu<sub>2</sub>O thin films.

#### **3.1 SILAR method**

The successive ionic layer Adsorption and Reaction (SILAR) method has been used to deposit Cu<sub>2</sub>O thin films. The SILAR method is a modified form of chemical bath deposition method (Paul Cartmell, 2011). SILAR requires the substrate to be immersed in chemical solution. Between each immersion the substrate is rinsed in purified water to get the desired coating over the substrate.

The SILAR method involves alternative immersion of the substrate in a solution containing a soluble salt of the cation and anion of the compounds to be deposited. The substrate supporting the growing film is rinsed in high purity deionized water after each immersion in order to avoid precipitation. In principle, SILAR is a deposition method in which thickness of the layer is determined by the number of deposition cycles. The SILAR method has been employed for the deposition of CdS, ZnS, CdZnS, PbS, CuS, CdSe, etc. thin films on different substrates. (Betul Guzeldir, et, al., 2010)

##### *3.1.2 Advantages of SILAR Method*

- ❖ Simple
  
- ❖ Less expensive. (Sankapal.B.R, et, al, .2000)

##### **3.1.3 Deposition parameters**

In SILAR method, solution concentration, pH, temperature of the precursors and immersion time are the important preparative parameters. In the present work temperature of the precursor solution is chosen as the variable deposition parameter.

## 3.2 Substrate Cleaning

The substrates are treated in  $\text{Cu}_2\text{O}$  an acidic bath containing Conc. nitric acid and Conc. hydrochloric acid in the ratio 1:3 for 2 hours. Then, the substrates are washed with extran soap solution. Finally the substrates are rinsed in deionised water and are dried in desiccators.

## 3.3 Deposition of the film

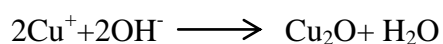
### 3.3.1 Chemicals used

Copper sulfate pentahydrate ( $\text{Cu SO}_4 \cdot 5\text{H}_2\text{O}$ ), sodium thio sulphate ( $\text{Na}_2 \text{S}_2 \text{O}_3 \cdot 5\text{H}_2\text{O}$ ) and sodium hydroxide ( $\text{NaOH}$ ) are used as the precursors for the deposition of  $\text{Cu}_2\text{O}$  thin film.

### 3.3.2 Preparation of $\text{Cu}_2\text{O}$ thin film

1M  $\text{NaOH}$  solution was prepared in a beaker. The copper thio sulphate is prepared by adding 1M sodium thio sulphate ( $\text{Na}_2 \text{S}_2 \text{O}_3 \cdot 5\text{H}_2\text{O}$ ) and 1M copper sulfate penta hydrate ( $\text{CuSO}_4 \cdot 5\text{H}_2\text{O}$ ) in the volumetric ratio of 5:1 with constant stirring for 5 minutes. Initially the temperature of the anionic solution is maintained at room temperature ( $30^\circ\text{C}$ ). No. of SILAR cycles under the adsorption /reaction time are maintained constant at 50 and 20 seconds respectively. To study the effect of temperature of the precursors samples are deposited by varying the temperature of anionic precursors. The substrate was immersed in the  $\text{NaOH}$  solution for 20 seconds. As a result,  $\text{OH}^-$  ions from  $\text{NaOH}$  solution get adsorbed to the surface of substrate. The substrate was immersed in the copper thio sulphate solution for 20 seconds. The reaction between  $\text{Cu}^+$  ion and  $\text{OH}^-$  ion takes place on the substrate surface leading to the formation of  $\text{Cu}_2\text{O}$ . After each immersion of substrate into cationic and anionic precursors the substrate were rinsed in a beaker containing deionized water.

The reaction occurring on the substrate surface can be represented as



The as- deposited films were annealed in air at  $200^\circ\text{C}$  and  $250^\circ\text{C}$ .

### 3.3.3 Film thickness

Film thickness is an important parameter that plays a role in the characterization of the film .Measurement of film thickness can be done in a number of ways.In the present work thickness of the films is measured by gravimetric method.

The film thickness is calculated using the equation,

$$t = m / \rho A$$

m- mass of the film

$\rho$  -density of the film.

A -Area of the film.

t - thickness of the film

### 3.4 Characterization

The structural characterization of the deposited film was carried out using X-ray diffractometer and scanning electron microscope (SEM). Optical transmittance was measured using a UV-Vis spectrophotometer.

#### 3.4.1 X- ray Diffraction (XRD)

X-ray Diffraction (XRD) is a powerful nondestructive technique for characterization of materials. It provides information on structures, phases, preferred crystal orientations (texture) and other structural parameters, such as average grain size, crystallinity, strain and crystal defects. X-ray diffraction peaks are produced by constructive interference of a monochromatic beam of X-rays scattered at specific angles from each set of lattice planes in a sample. The peak intensities are determined by the atomic arrangements within the lattice planes.

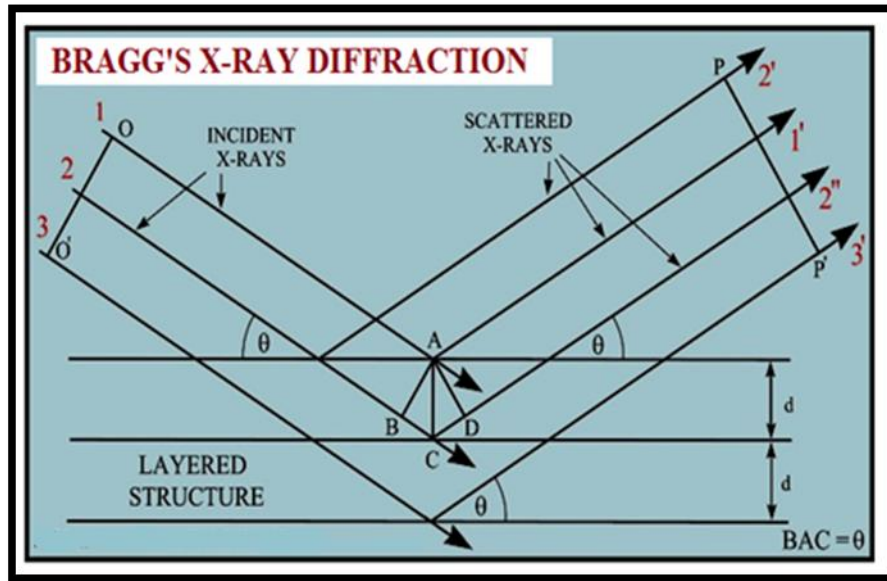


figure 3.1 Schematic diagram of X-ray diffraction

The basic principle behind X- ray diffraction is Bragg Law

$$n\lambda = 2d \sin\theta$$

Where,

$\lambda$  is the wavelength of the X-Rays.

$n$  is the order of diffraction.

$d$  is the distance between different planes of atoms in the crystal lattice.

$2\theta$  is the angle of diffraction.

The lattice parameter ( $a$ ) is calculated from the relation

$$d = a / (h^2 + k^2 + l^2)^{1/2}$$

$d$  is the inter planner spacing.

$h, k, l$  – Miller indices.

The crystallite size was calculated from X ray diffraction peak broadening using the Scherrer formula.

$$D = k\lambda / \beta \cos\theta$$

$\lambda$  is the wavelength of X-rays,  $k$  is the scherrer constant,  $\beta$  is the full width at half maximum intensity of the diffraction peak for which the particle size is to be calculated,  $2\theta$  is the diffraction angle of the concerned diffraction peak and  $D$  is the crystallite size.

### 3.4.2 Scanning Electron Microscopy (SEM)

The SEM uses **electrons** for imaging, much as a light microscope uses visible light. The scanning electron microscope (SEM) uses a focused beam of high-energy electrons to generate a variety of signals at the surface of solid specimens. The signals that derive from electron-sample interactions reveal information about the sample including external morphology (texture), chemical composition and crystalline structure and orientation of materials making up the sample. The SEM is also capable of performing analyses of selected point locations on the sample; this approach is especially useful in qualitative or semi-quantitative determination of chemical compositions, crystalline structure and crystal orientations. The advantages of SEM over light microscopy include higher magnification and greater depth of field (up to 100 times that of light microscopy).

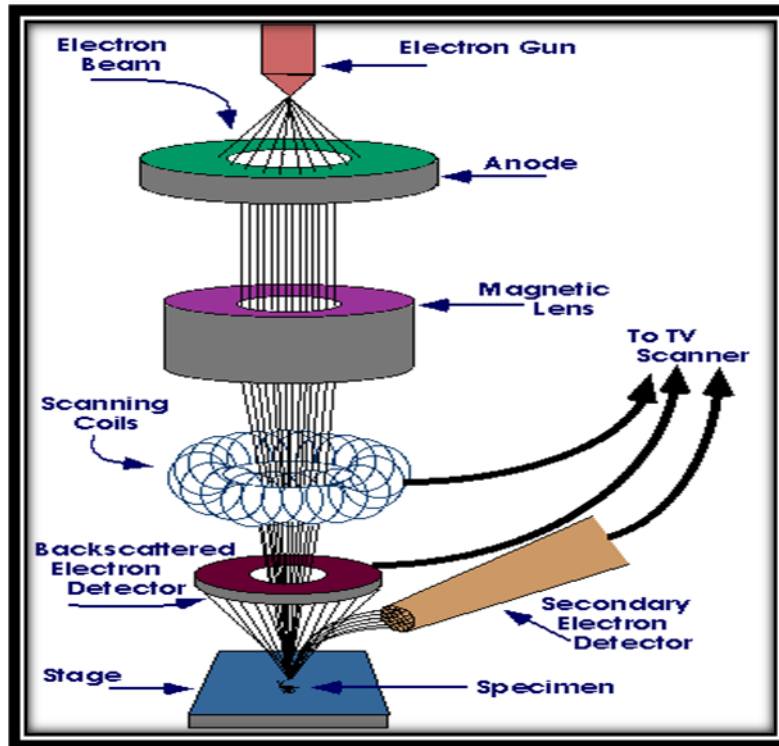


Figure 3.2. schematic diagram of the scanning electron microscope.

Accelerated electrons in a SEM carry significant amounts of kinetic energy and this energy is dissipated as a variety of signals produced by electron-sample interactions when the incident electrons are decelerated in the solid sample. These signals include secondary electrons (that produce SEM images), back scattered electrons (BSE), diffracted back scattered electrons (EBSD that are used to determine crystal structures and orientations of minerals), photons (characteristic X-rays that are used for elemental analysis and continuum X-rays), visible light (cathodoluminescence CL) and heat. Secondary electrons and backscattered electrons are commonly used for imaging samples: secondary electrons are most valuable for analyzing morphology and topography of samples and backscattered electrons are most valuable for illustrating contrasts in composition in multiphase samples. X-rays are produced by inelastic collisions of the incident electrons with electrons in discrete shells of atoms in the sample. As the excited electrons return to lower energy states, they yield X-rays that are of a fixed wavelength (that is related to the difference in energy levels of electrons in different shells for a given element). Thus, characteristic X-rays are produced for each element in a mineral that is "excited" by the electron beam. SEM analysis is considered to be "non-destructive"; that is, X-rays generated

by electron interactions do not lead to volume loss of the sample, so it is possible to analyze the same materials repeatedly.

### 3.4.3 UV- Visible spectroscopy

The principle of UV/visible spectroscopy is the excitation of electrons to higher energetic molecular orbital's because of absorption of UV/ visible radiation .UV Visible spectroscopy measures the response of a sample to ultraviolet and visible range of electromagnetic radiations. Ultraviolet and visible radiation interacts with matter which causes electronic transitions (promotion of electrons from the ground state to a high energy state).

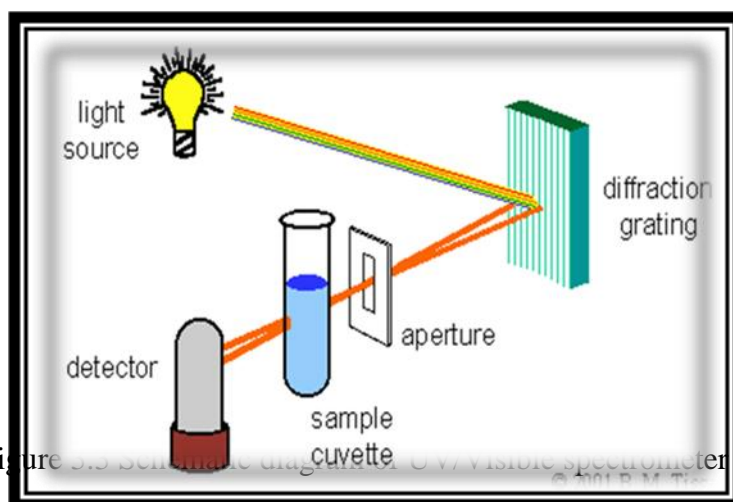


Figure 3.3 Schematic diagram of UV/ visible spectrometer

Absorption of visible and ultraviolet (UV) radiation is associated with excitation of electrons, in both atoms and molecules, from lower to higher energy levels. Since the energy levels of matter are quantized, only light with the precise amount of energy can cause transitions from one level to another level. The absorption coefficient ( $\alpha$ ) is related to the extinction coefficient ( $k$ ) by the following equation

$$\text{Absorption coefficient } \alpha = 4\pi k / \lambda$$

$k$  is calculated by the following formula

$$k = 2.303 \cdot \lambda \log (1/t) / 4\pi d$$

$\lambda$  is the wavelength of electromagnetic radiation.

Table-3.3 Film deposition conditions

TEMPERATURE OF THE ANIONIC PRECURSOR (°C)	IMMERSION TIME (SECONDS)	NUMBER OF SILAR CYCLES	THICKNESS OF THIN FILM ( $\mu\text{m}$ )
30	20	50	0.496
50	20	50	0.61
70	20	50	0.524

## CHAPTER-4

### RESULTS AND DISCUSSION

Cuprous oxide thin films are deposited by SILAR method. The deposited Cu<sub>2</sub>O films are characterized by X- ray diffraction, scanning electron microscope, UV/Visible spectroscopy. The properties of the films are investigated as a function of the temperature of precursor solution.

#### 4.1 Structural properties

Figures 4.1 to 4.9 show that XRD patterns of as-deposited and annealed Cu<sub>2</sub>O thin films, respectively.

As deposited films of sample 1 is amorphous in nature and the crystallinity of the films improved with annealing. Cu<sub>2</sub>O thin films annealed at 250<sup>0</sup>c exhibited prominent peaks. The peak position and relative intensities are compared with the standard data (JC PDS–05-0667). The film exhibited broad diffraction peak of very low intensity at  $2\theta = 35.5$  and  $38.7$ .

Crystallite size is calculated from XRD data using Debye Scherrer relation and the calculated crystallite size are reported in table 4.1. The crystallinity of the films improved, when the bath temperature is increased and the film deposited at a high temperature exhibit very broad diffraction indicating the formation of polycrystalline material.

S. R. Yoganaranrasimhan and C. N. Rao, (1996) reported that the grain size strongly dependent on the annealing temperature.

#### 4.2 Morphology

SEM images of the Cu<sub>2</sub>O thin film sample 2 annealed at 250<sup>0</sup>C is shown in figure 4.10. Scanning electron micrograph reveals that the deposition is uniform and deposit is porous in nature.

## 4.3 Optical properties

### 4.3.1 Transmittance

Optical transmittance spectra of Cu<sub>2</sub>O thin film shown in figure 4.12 to 4.13, the transmittance of the film decreased with decreasing wavelength the film exhibited higher transmittance in longer wavelength region. The film exhibited a transmittance of 40% at 1200nm. With increase in bath temperature the transmittance of the films decreases. Transmittance of the films increases with annealing. The result agrees well with the observation of (M.Mahaboob Beevi et al., 2010)

### 4.3.2 Absorbance

Optical absorbance spectra of Cu<sub>2</sub>O thin film shown in figure 4.14 to 4.16, the absorbance of the film decreased with increasing wavelength the film exhibited lower absorbance in longer wavelength region. The film exhibited low absorbance at 1200nm. With increase in bath temperature the absorbance of the films increase. Absorbance of the films increases with annealing. This is in good agreement with results reported by (R.A.Chikwenze and M.N. Nnabuchi, 2010).

### 4.3.4 Band gap

Optical band gap of the films is calculated from  $(\alpha h\nu)^2$  vs photon energy ( $h\nu$ ). The optical band gap of the film varied from 2.3-1.6 eV on varying the temperature of precursor solution. The film deposited at a precursor solution temperature of 70<sup>0</sup>C recorded a minimum band gap. which match approximately well with the reported by (Rodrigo Cue S. et al., 2009). Energy band gap ( $E_g$ ) values for Cu<sub>2</sub>O are shown in Table 4.2

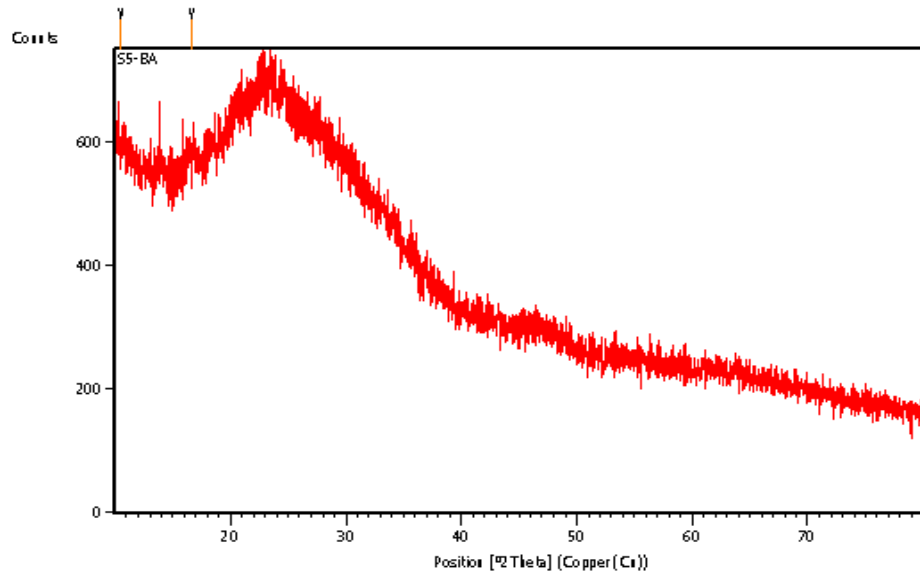


Figure 4.1 XRD pattern of as-deposited  $\text{Cu}_2\text{O}$  thin film Sample 1

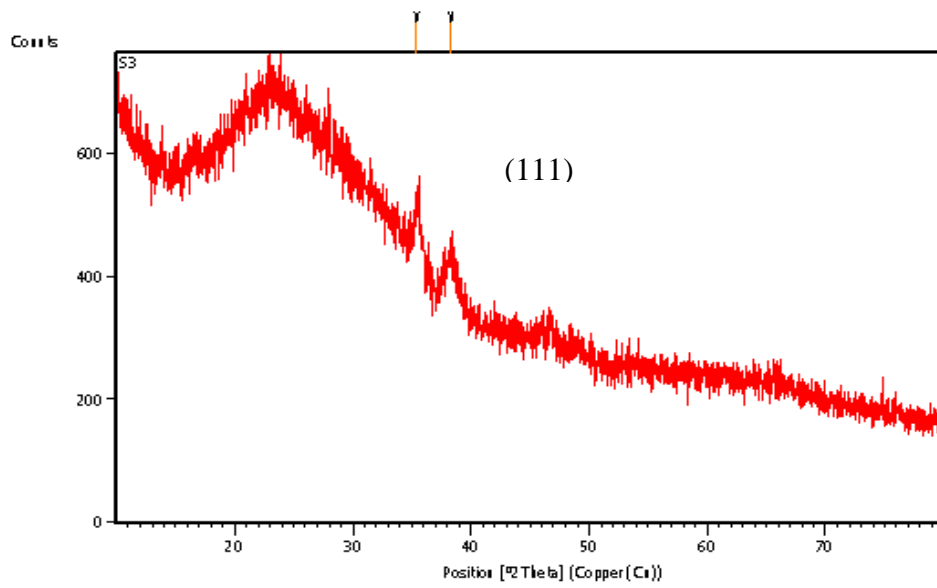


Figure 4.2, XRD pattern of as-deposited  $\text{Cu}_2\text{O}$  thin film Sample 2

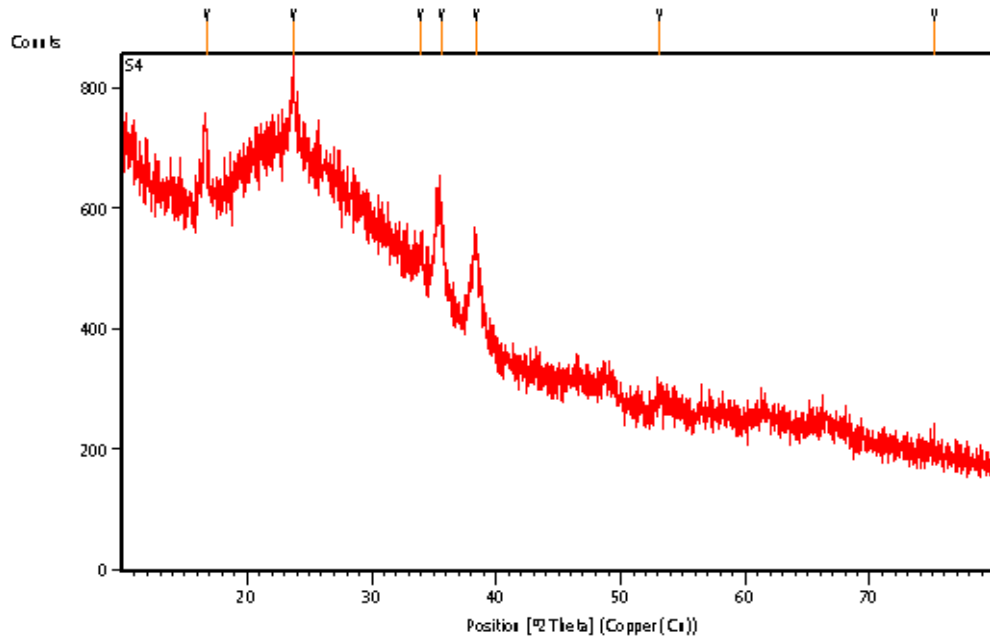


Figure 4.3, XRD pattern of as-deposited  $\text{Cu}_2\text{O}$  thin film Sample 3

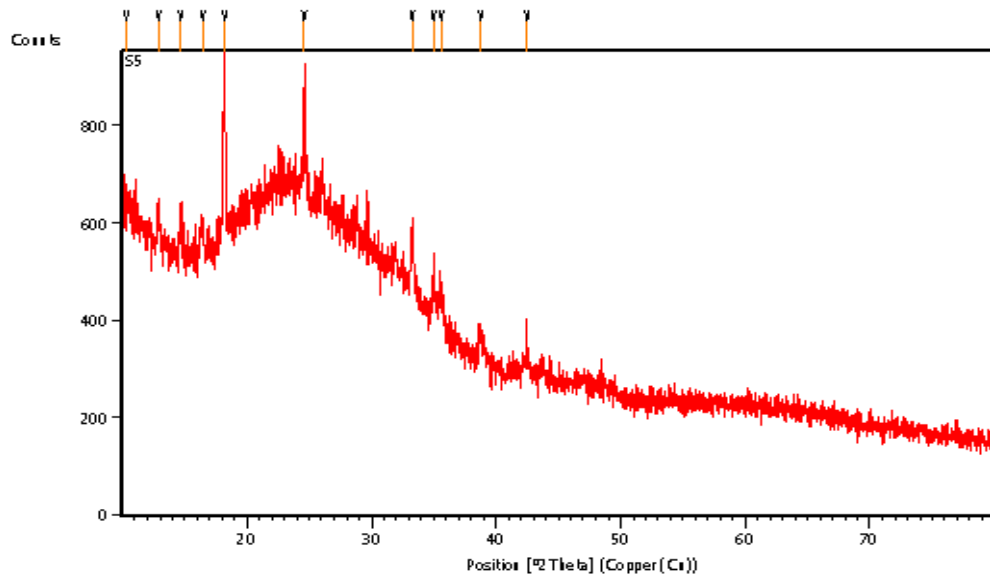


Figure 4.4 XRD pattern of annealed ( $200^\circ\text{C}$ )  $\text{Cu}_2\text{O}$  thin film Sample 1

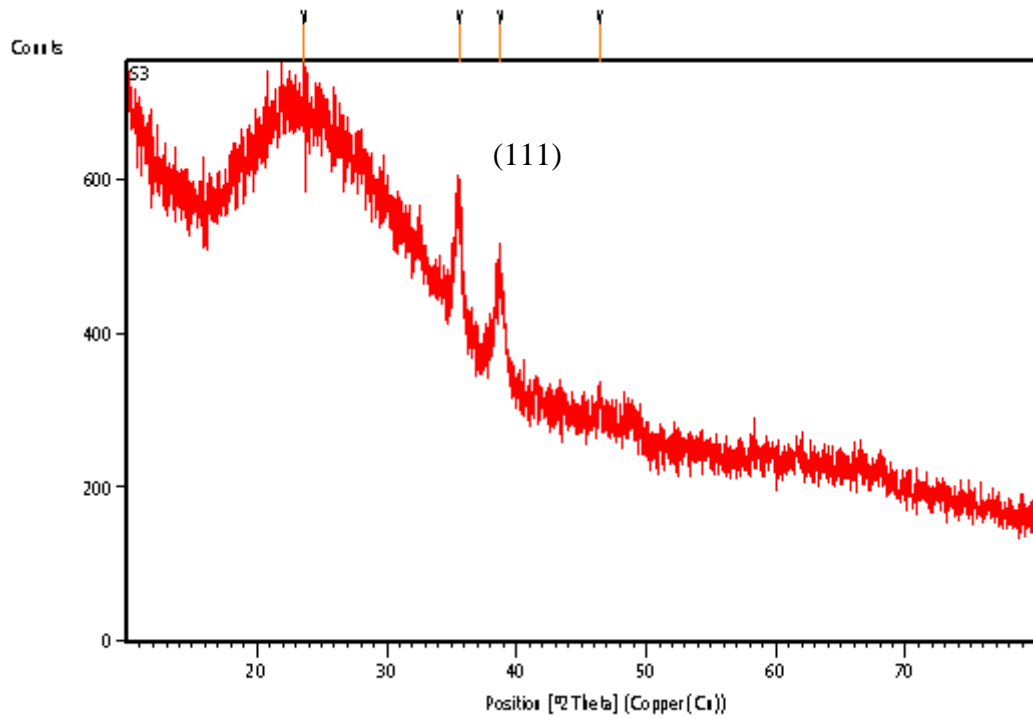


Figure 4.5 XRD pattern of annealed (200°C) Cu<sub>2</sub>O thin film Sample 2

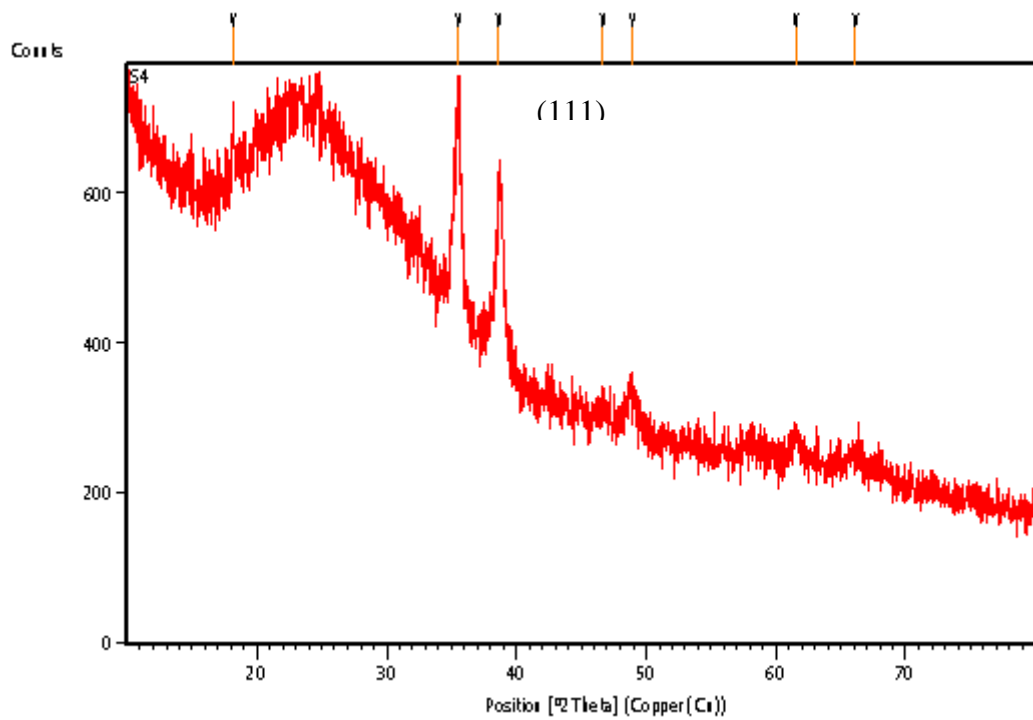


Figure 4.6 XRD pattern of annealed (200<sup>0</sup>C) Cu<sub>2</sub>O thin film Sample 3

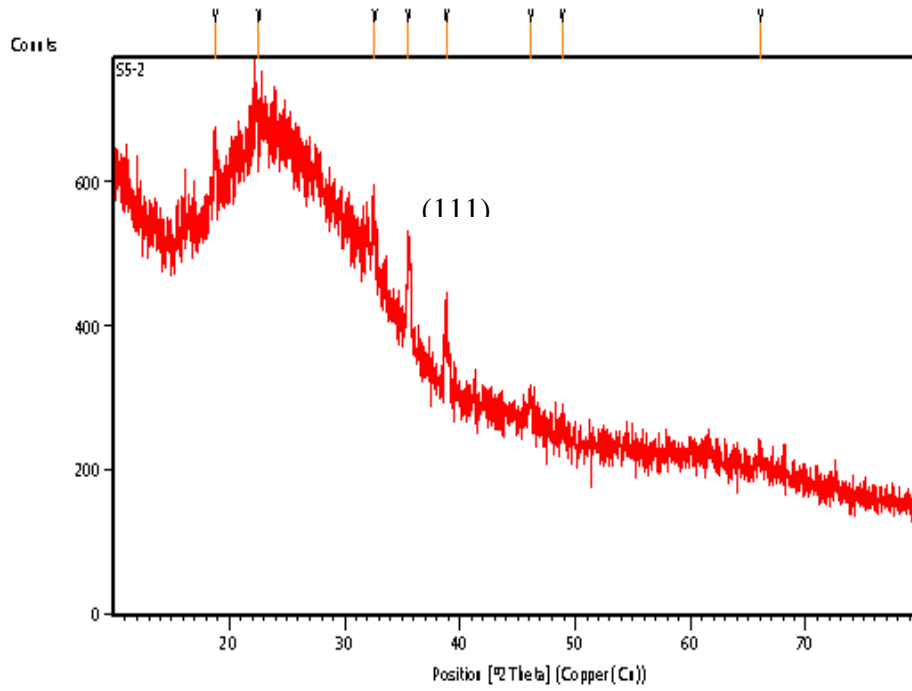


Figure 4.7 XRD pattern of annealed (250<sup>0</sup>C) Cu<sub>2</sub>O thin film Sample 1

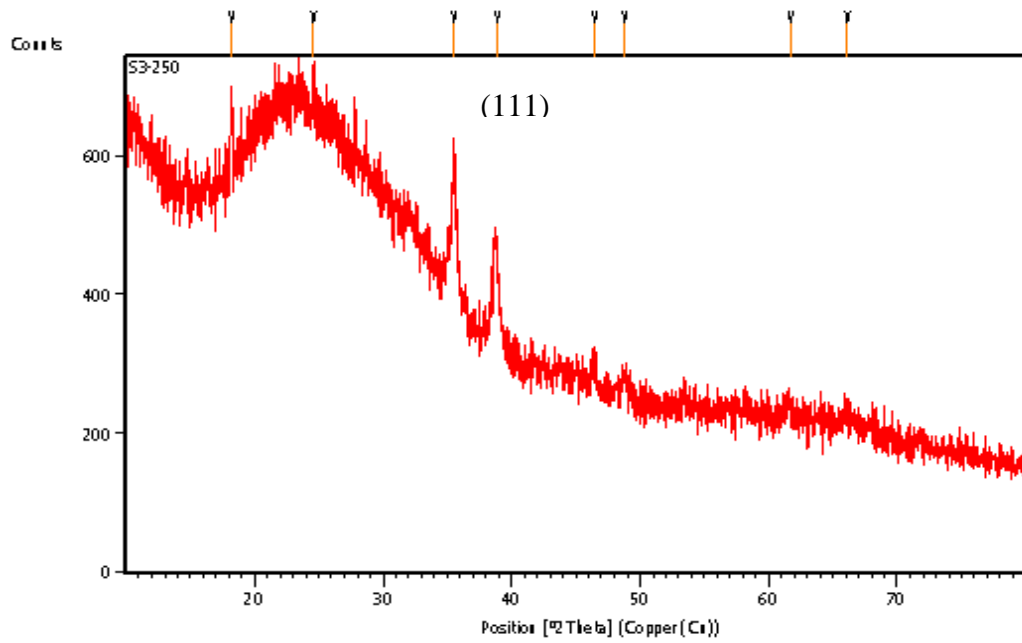


Figure 4.8 XRD pattern of annealed (250<sup>0</sup>C) Cu<sub>2</sub>O thin film Sample 2

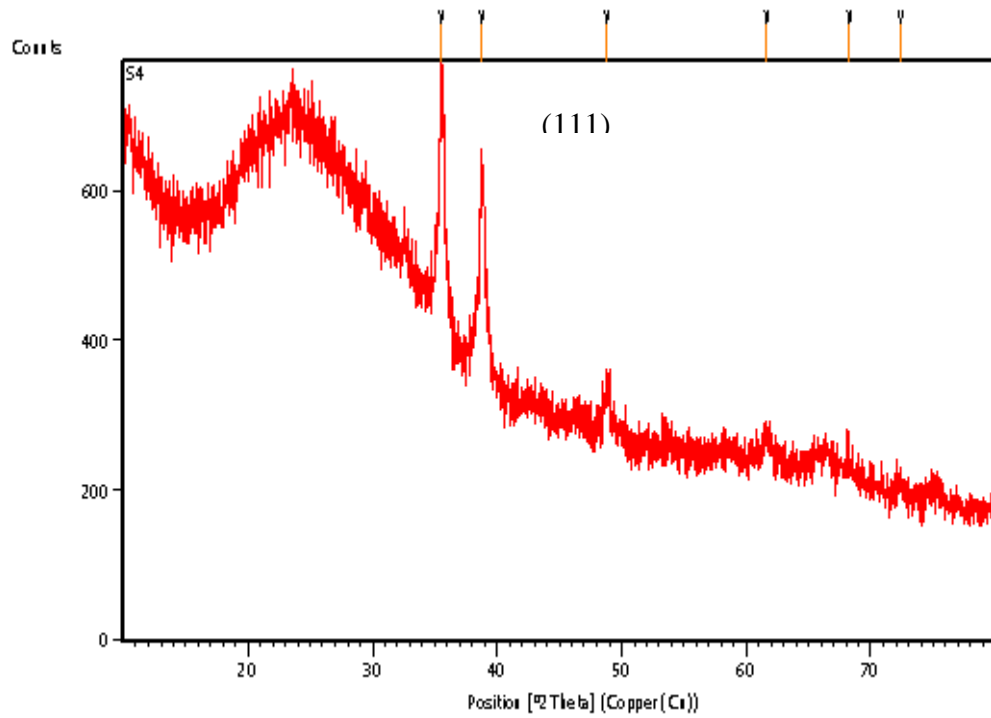


Figure 4.9 XRD pattern of annealed (250<sup>0</sup>C) Cu<sub>2</sub>O thin film Sample 3

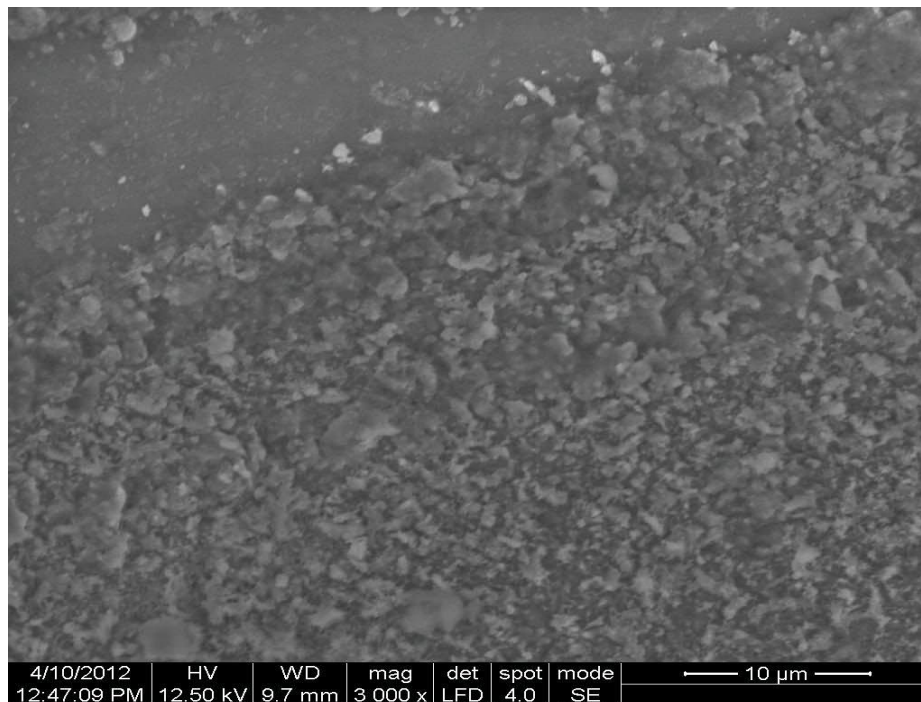


Figure 4.10:a) Scanning electron micrograph of Cu<sub>2</sub>O thin film (sample 2 annealed at 250<sup>0</sup>C)

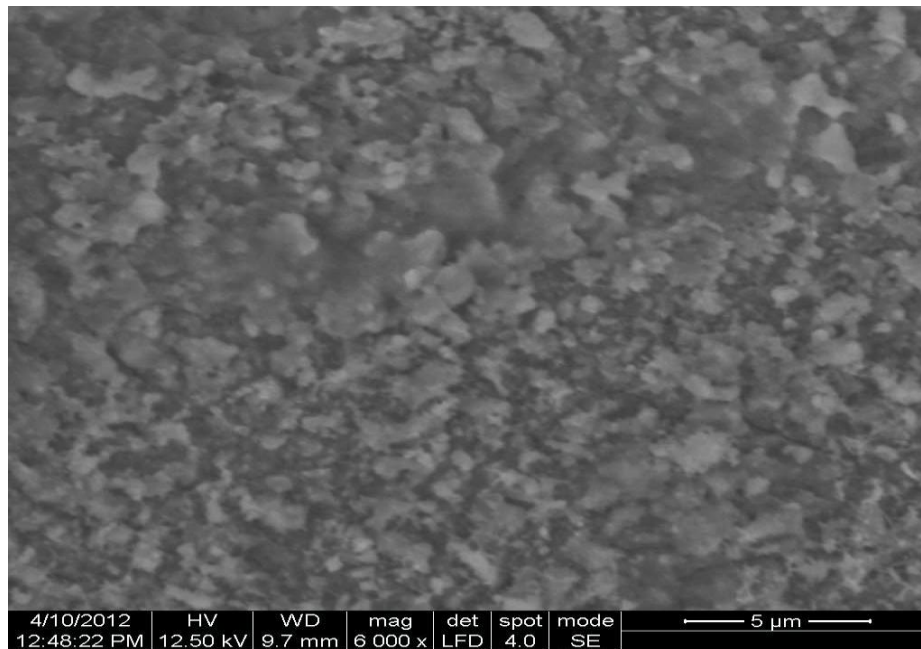


Figure 4.10: b) Scanning electron micrograph of  $\text{Cu}_2\text{O}$  thin film (sample 2 annealed at  $250^\circ\text{C}$ )

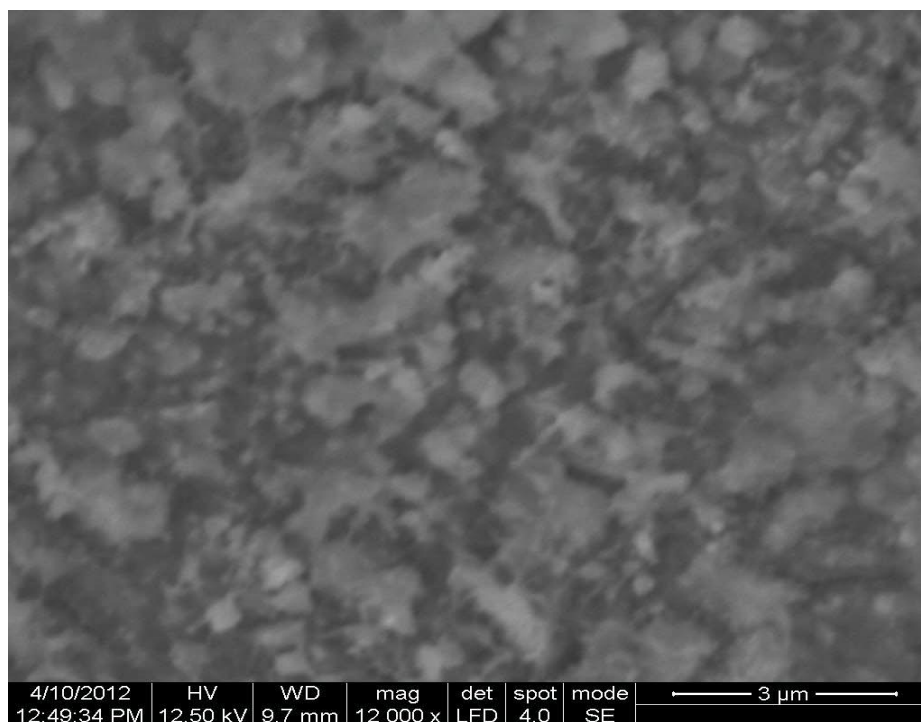


Figure 4.10:c) Scanning electron micrograph of  $\text{Cu}_2\text{O}$  thin film (sample 2 annealed at 250)

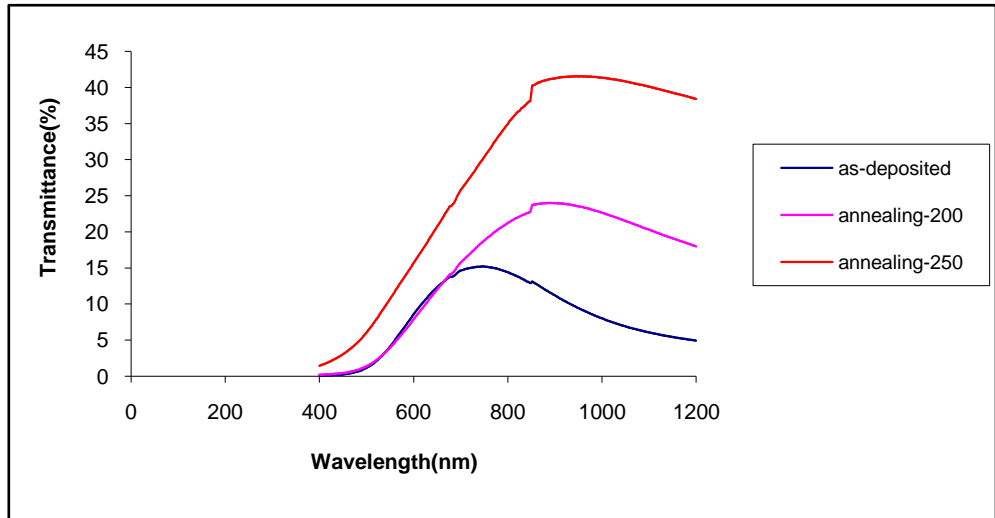


Figure 4.11 optical transmittance ( $T$ ) spectra of as-deposited and annealed  $\text{Cu}_2\text{O}$  thin film sample 1

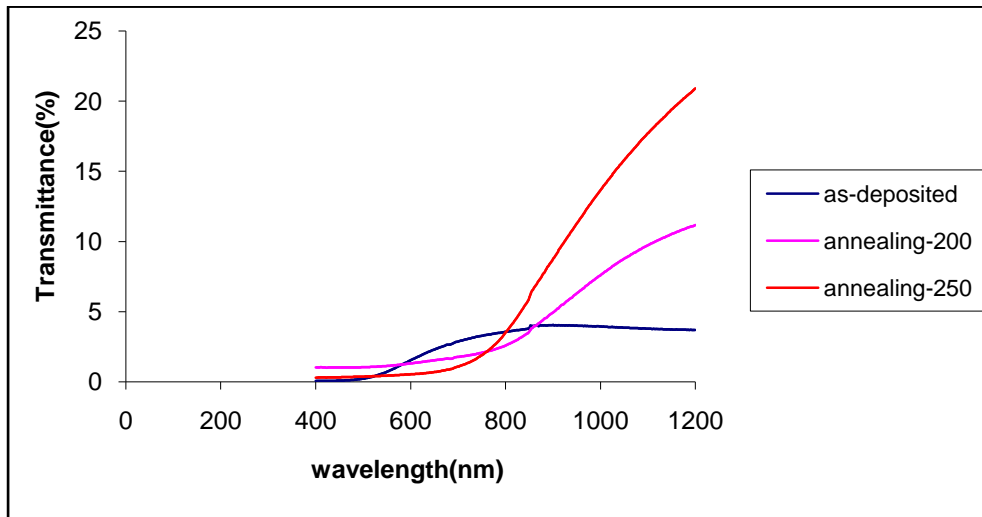


Figure 4.12 optical transmittance ( $T$ ) spectra of as-deposited and annealed  $\text{Cu}_2\text{O}$  thin film sample 2

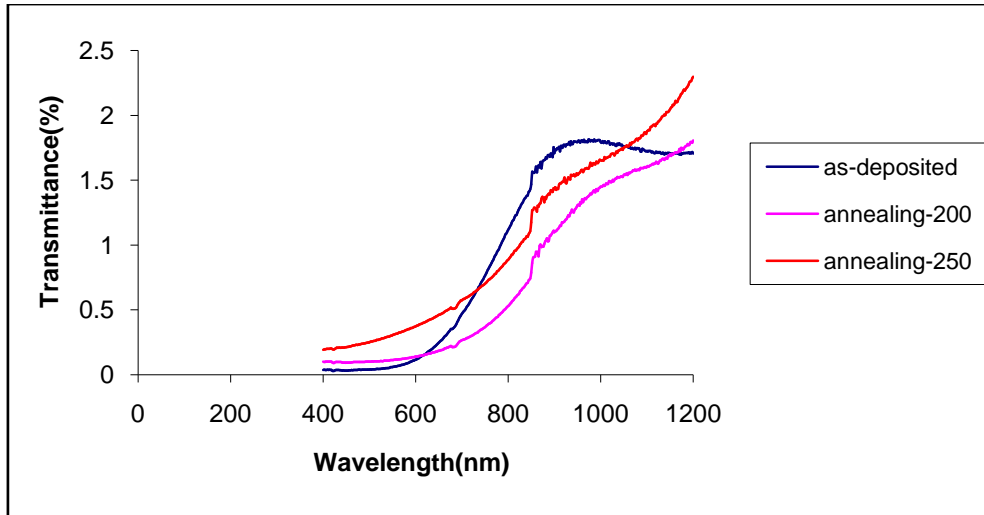


Figure 4.13 optical transmittance (T) spectra of as-deposited and annealed  $\text{Cu}_2\text{O}$  thin film sample3

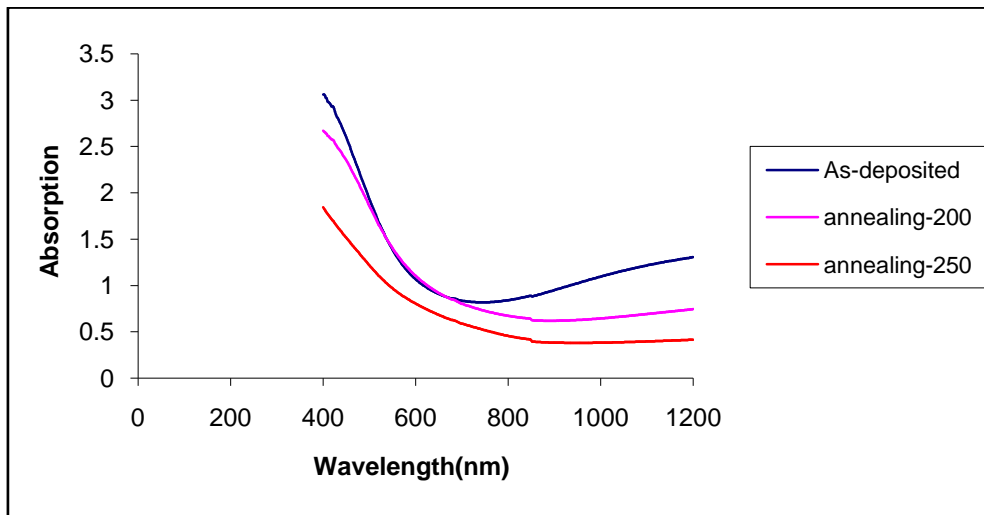


Figure 4.14 optical absorption spectra of as-deposited and annealed  $\text{Cu}_2\text{O}$  thin film sample1

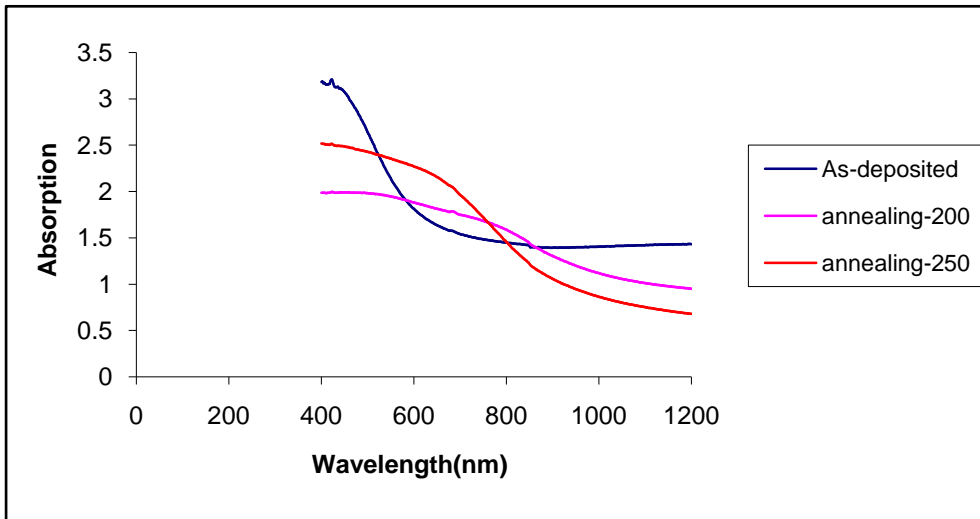
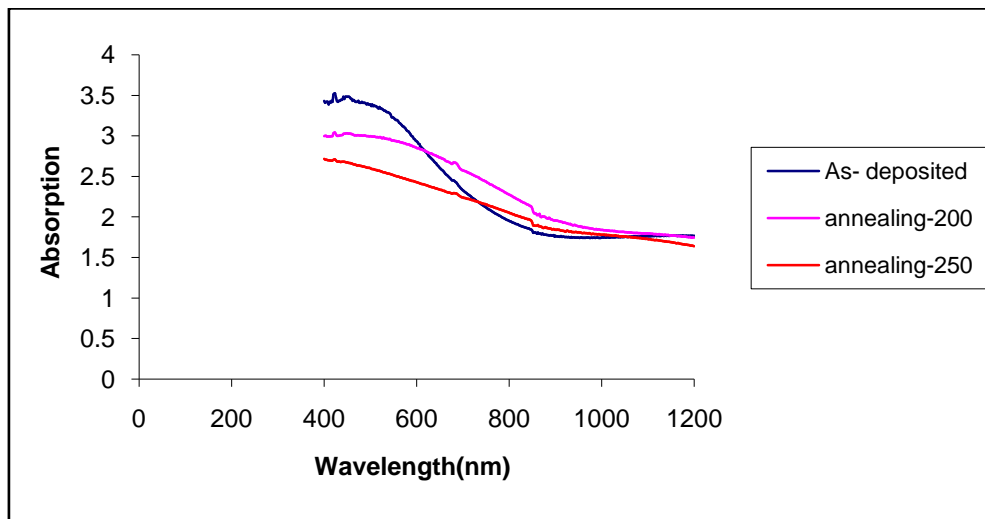


Figure 4.15 optical absorption spectra of as-deposited and annealed  $\text{Cu}_2\text{O}$  thin film sample2



. Figure 4.16 optical absorption spectra of as-deposited and annealed  $\text{Cu}_2\text{O}$  thin film sample3

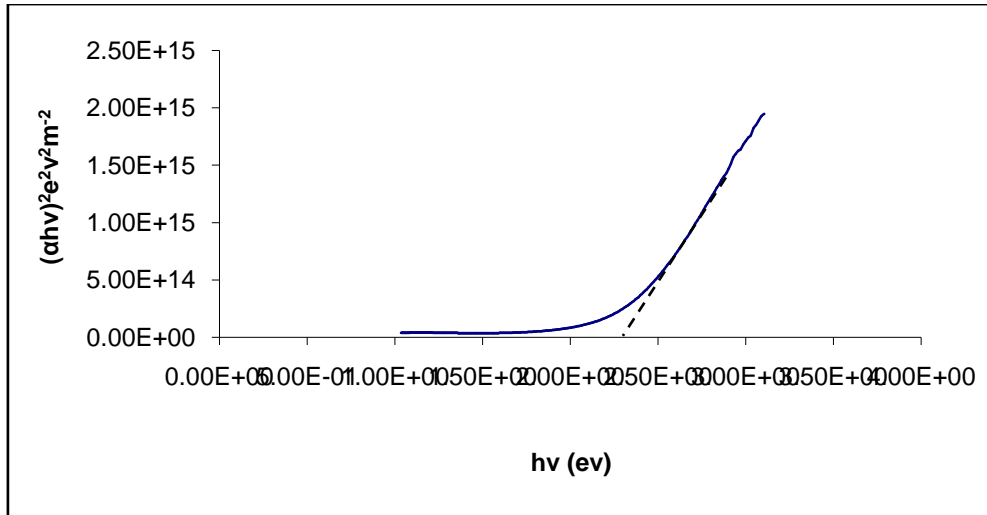


Figure 4.17  $(\alpha h\nu)^2$  vs.  $(h\nu)$  Plot of as-deposited  $\text{Cu}_2\text{O}$  thin film sample 1

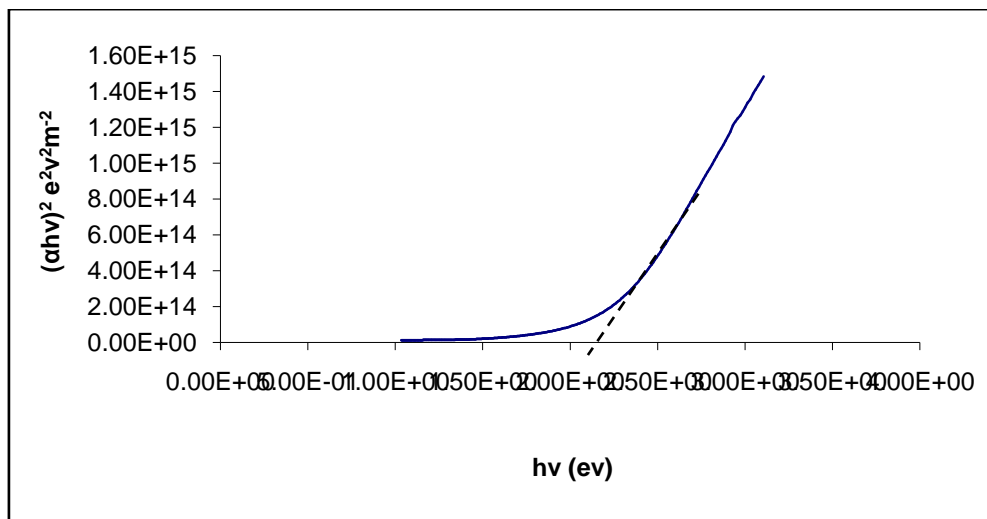


Figure 4.18  $(\alpha h\nu)^2$  vs.  $(h\nu)$  Plot of annealed ( $200^\circ\text{C}$ )  $\text{Cu}_2\text{O}$  thin film sample 1

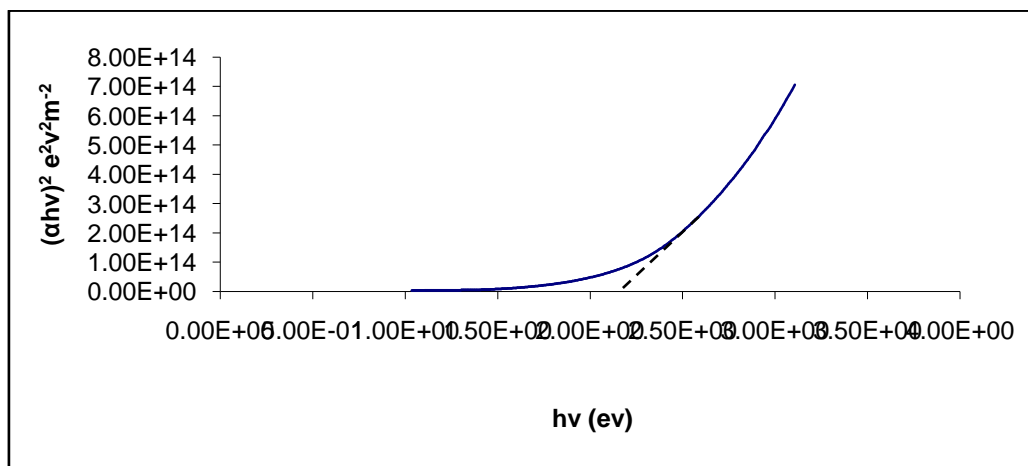


Figure 4.19  $(\alpha h\nu)^2$  vs.  $(h\nu)$  plot of annealed (250<sup>0</sup>C) Cu<sub>2</sub>O thin film sample1

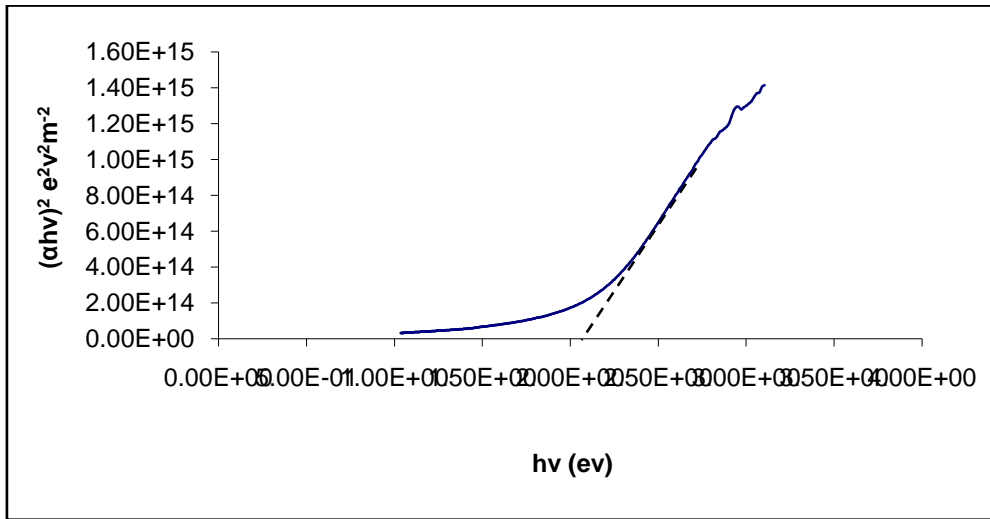


Figure 4.20  $(\alpha h\nu)^2$  vs.  $(h\nu)$  plot of as-deposited Cu<sub>2</sub>O thin film sample2

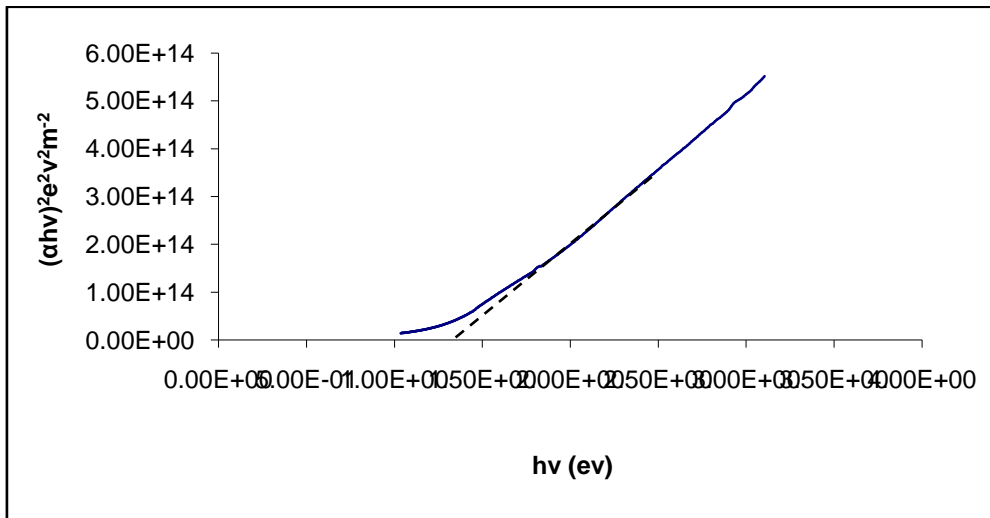


Figure 4.21  $(\alpha h\nu)^2$  vs.  $(h\nu)$  plot of annealed (200<sup>0</sup>C) Cu<sub>2</sub>O thin film sample2

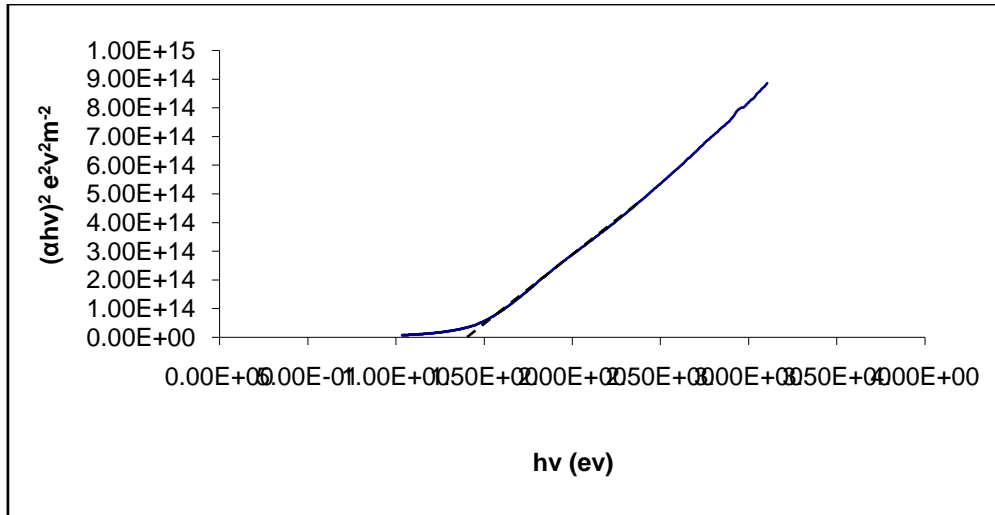


Figure 4.22  $(\alpha h\nu)^2$  vs.  $(h\nu)$  plot of annealed ( $250^\circ\text{C}$ )  $\text{Cu}_2\text{O}$  thin film sample2

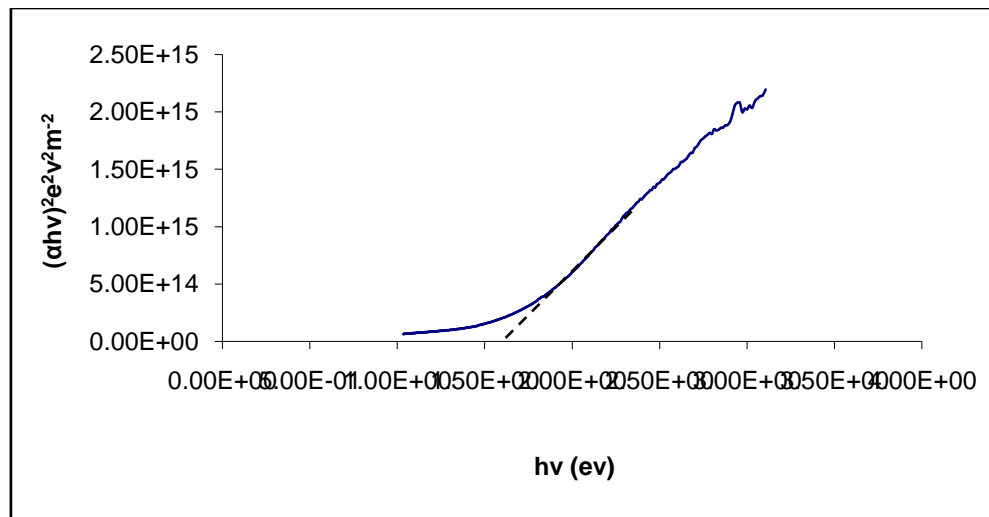


Figure 4.23  $(\alpha h\nu)^2$  vs  $(h\nu)$  Plot of as-deposited  $\text{Cu}_2\text{O}$  thin film sample3

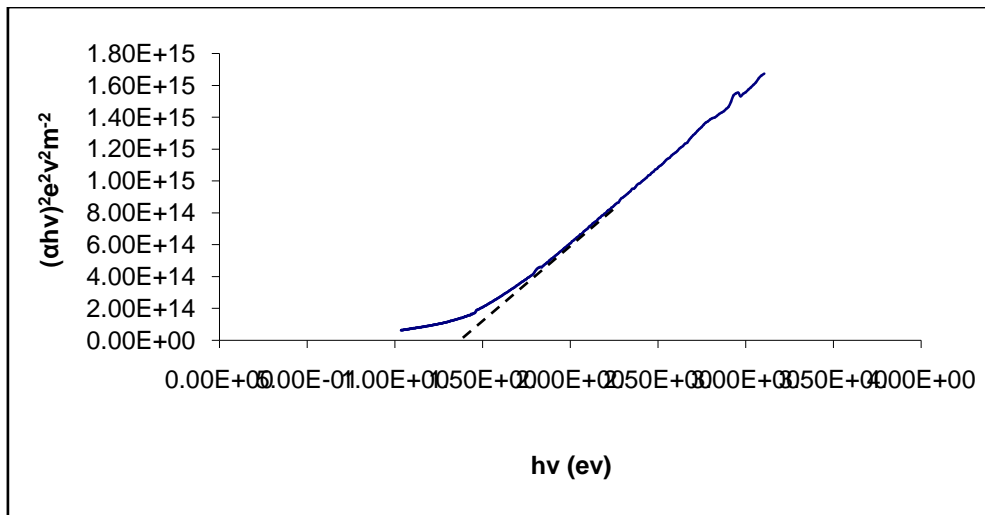


Figure 4.24  $(\alpha h\nu)^2$  vs  $(h\nu)$  Plot of annealed ( $200^\circ\text{C}$ )  $\text{Cu}_2\text{O}$  thin film sample3

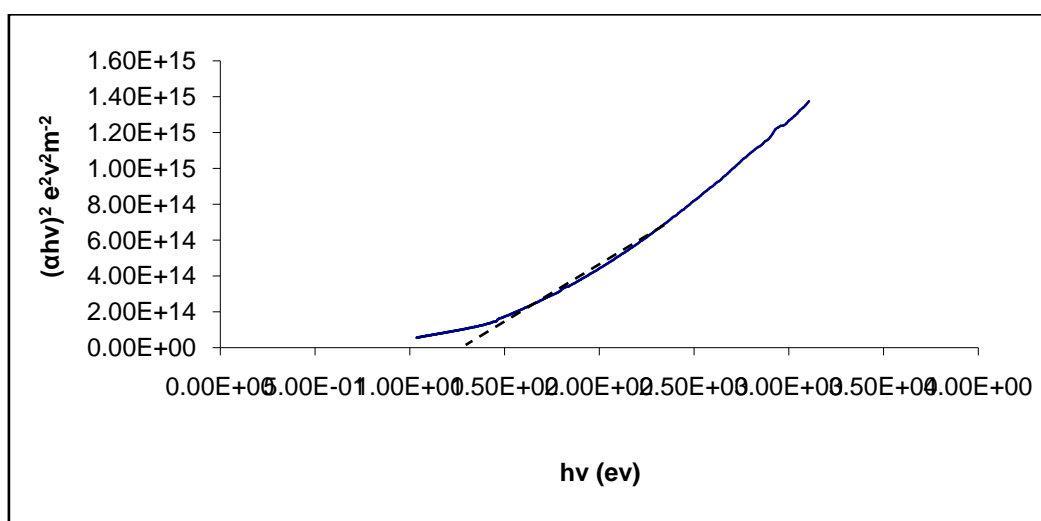


Figure 4.25  $(\alpha h\nu)^2$  vs  $(h\nu)$  Plot of annealed ( $250^\circ\text{C}$ )  $\text{Cu}_2\text{O}$  thin film sample3

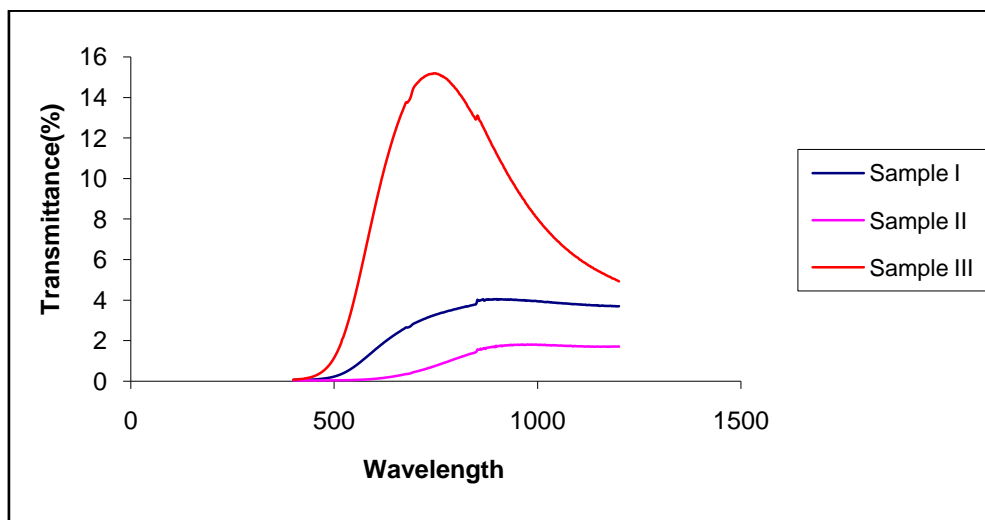


Figure 4.26: variation of transmittance with wave length of  $\text{Cu}_2\text{O}$  thin film

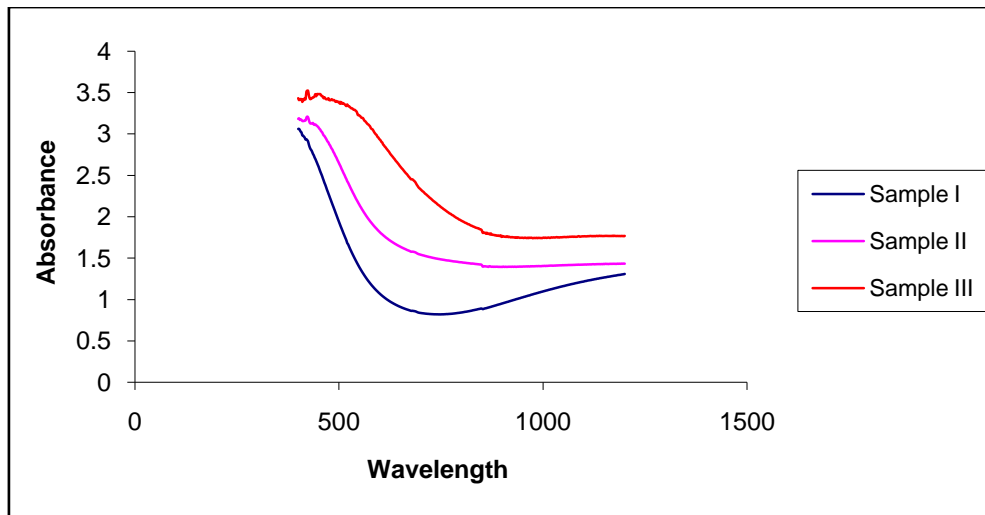


Figure 4.27: variation of absorption with wave length of  $\text{Cu}_2\text{O}$  thin film

Table 4.1-Grain size of  $\text{Cu}_2\text{O}$  thin film

Sample code	Temperature of the precursor solution( <sup>0</sup> C)	Thickness ( $\mu\text{m}$ )	Grain size (nm)		
			As-DEPOSITED	Annealing	
				200 <sup>0</sup> C	250 <sup>0</sup> C
1	30	0.496		29.7	41.57
2	50	0.605	20.78	38.25	47.896
3	70	0.524	35.63	42.54	49.87

Table 4.2 Energy band gap ( $E_g$ ) for  $\text{Cu}_2\text{O}$  thin film

Samples	Temperature ( <sup>0</sup> C)	Energy Band Gap (eV)		
		As- Deposited	<b>Annealing</b>	
			200 <sup>0</sup> c	250 <sup>0</sup> c
1	30	2.3	2.2	2.15
2	50	2.05	1.35	1.4
3	70	1.6	1.4	1.35

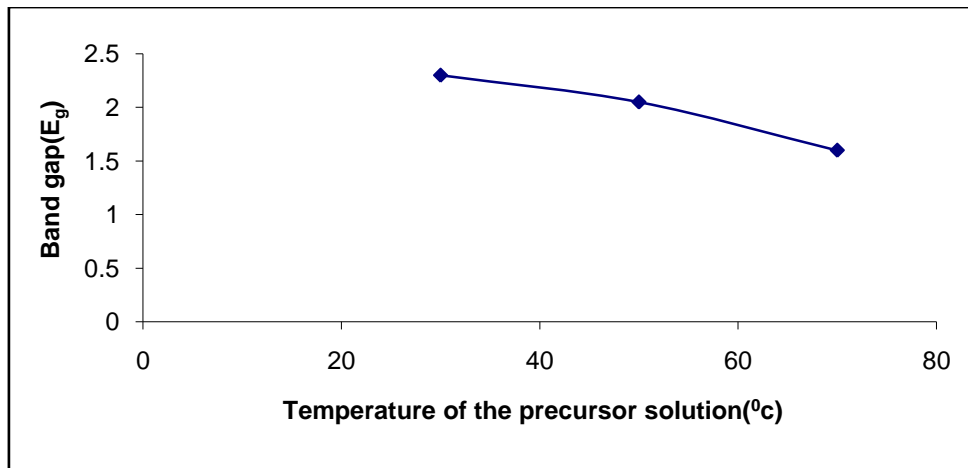


Figure 4.28: variation of band gap with temperature of the precursor solution of  $\text{Cu}_2\text{O}$  thin film(as deposited)

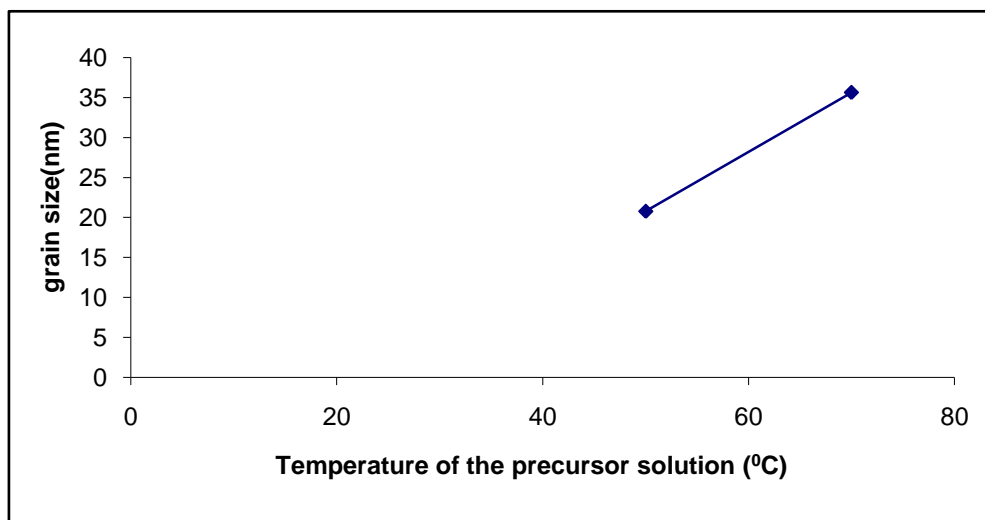


Figure 4.29: variation of grain size with temperature of the precursor solution of  $\text{Cu}_2\text{O}$  thin film(as deposited)

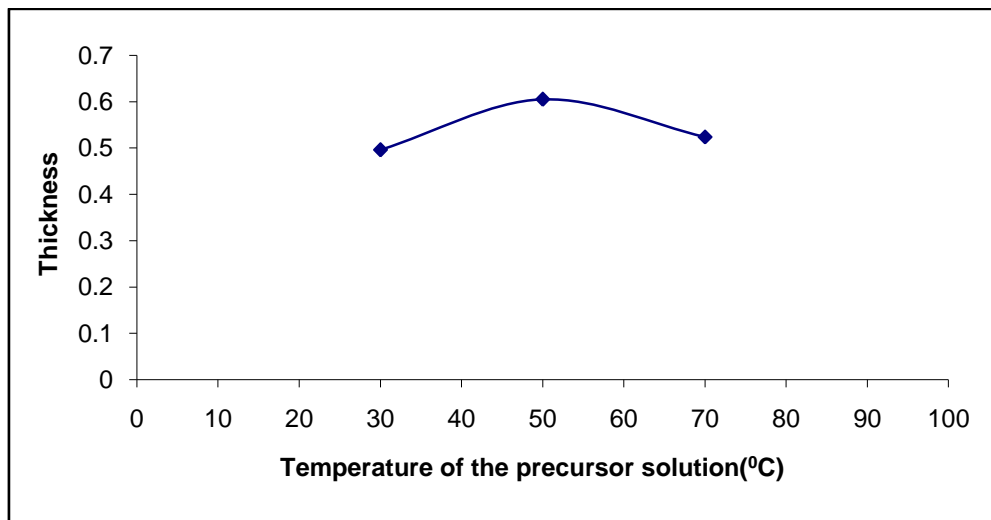


Figure 4.30: variation of thickness with temperature of the precursor solution of  $\text{Cu}_2\text{O}$  thin film (as deposited)

## PLATE I

### Experimental set up of SILAR Deposition Method



## CHAPTER-5

### SUMMARY AND CONCLUSION

The SILAR method is simple and inexpensive, which comprises excellent material utilization efficiency, good control over deposition process along with film thickness and it is a convenient method for large area deposition on substrate.

In the present work an attempt has been made to study the effect of temperature of the precursor solution on the structural, optical and morphological properties of  $\text{Cu}_2\text{O}$  film. The structural studies showed that as deposited  $\text{Cu}_2\text{O}$  thin films are amorphous in nature and the crystallinity was improved with bath temperature. Scanning Electron micrograph shows that the deposition is uniform. The annealed film had a porous microstructure.

The  $\text{Cu}_2\text{O}$  film annealed at  $250^\circ\text{C}$  shows higher transmittance. The optical band gap of the films is found to decrease with increasing temperature of the precursor solution.

## REFERENCES

1. P. E. de Jongh,\* D. Vanmaekelbergh, and J. J. Kelly, 1999 ,Chem. Mater. volume:11 , Pg: 3512–3517
2. T Mahalingam, J.S.P Chitra, S Rajendran ,M Jayachandran, Mary Juliana Chockalingam, 2000.Journal of Crystal Growth,volume:216, Pg: 304–310
3. Jaeyoung Lee, and Yongsug Tak, 2000, Electrochemical and Solid-State Letters, volume: 3, Pg:69-72
4. V. Georgieva , M. Ristov ,2001, Solar Energy Materials & Solar Cells, volume:73, Pg: 67–73
5. Sekhar C. Ray, 2001, solar energy materials& solar cells, Volume 68,Pg: 307-312
6. Jorge Medina-Valtierra , Jorge Ram´irez-Ortiz ,Victor M. Arroyo-Rojas , Facundo Ruiz , 2002 , Applied Catalysis A: General, volume –238 ,Pg: 1–9
- 7.T Mahalingam, J S P Chitra, S Rajendran and P J Sebastian, 2002  
Semiconductor science and technology, Volume: 17,Pg: 6
8. M. Ristov, Gj. Sinadinovski, I. Grozdanov, 2002, Thin Solid Films, Volume 123, Pg 63–67.
9. A.P. Chatterjee, A.K. Mukhopadhyay, A.K. Chakraborty, R.N. Sasmal, S.K. Lahiri, 2003, Materials Letters, Volume: 11, Pg: 358–362
10. T. Mahalingam, J.S.P Chitra,G.Ravi,J.P Cha.P.J.Sebastian, 2003, Surface and Coatings Technology, volume:168, Pg: 111–114
11. Ivan Grozdanov, 2003, Materials Letters,volume: 19, Pg: 281–285
12. D.D.O. Eya, A.J. Ekpunobi, and C.E. Okeke, FAS, 2005, The Pacific Journal of Science and Technology ,2005, Volume:6,Pg:246-250
13. T. Mahalingam, J.S.P. Chitra, J.P. Chu,S. Velumani, P.J. Sebastian, 2005, Solar Energy Materials and Solar Cells,volume:88, Pg: 209–216

14. K. Akimoto , S. Ishizuka, M. Yanagita, Y. Nawa, Goutam K. Paul, T. Sakurai , 2006, Solar Energy, Volume :80, Pg: 715-722.
15. Yueh-Hsun Lee ,Ing-Chi Leu, Cheng-Lung Liao, Kuan-Zong Fung, 2006, Journal of Alloys and Compounds,Volume 436, Pg: 241–246
16. Xun Li, Feifei Tao, Yuan Jiang, Zheng Xu, 2007, Journal of Colloid and Interface Science, volume: 308, Pg: 460–465
17. R. Neskovska ,M. Ristova ,J. Velevska , M. Ristov , 2007, Thin solid films, Volume: 515, Pg: 4717–4721
18. Seong Ho Jeong, Erays. Aydil, 2009, Journal of Crystal Growth, Volume: 311, Pg: 4188–4192
19. Long-cheng Wang, Hong Jia, Ling-yun Shi, Na Liao, Xiao-jing Yu and Da-lai Jin, 2009, inorganic materials ,volume:46, Pg: 847-851
20. SeongHo Jeong and Eray S. Aydil , 2010, Journal of Vacuum Science & Technology , Volume 2, Pg:456-460
21. MuhammadMuhibbullah and Masaya Ichimura, 2010, Japanese Journal of Applied Physics, volume: 49,Pg: 657-660
22. Lila Chaal, Catherine Debiemme-Chouvy, Claude Deslouis, Georges Maurin, Alain Pailleret Boualem Saidani, 2010, Surface Science, Volume 605, Pg: 121–130,
23. Prakash Bansilal Ahirrao, D. R. Patil, Sanjay S. Sonawane, M. S. Shinde, R. S. Patil, 2010, Journal of Scientific Review, volume: 2, Pg: 86-90
24. Xiao Jiao Yu, A Man Zhang, Jian Zhang, Jie Zhao, Bing Hua Yao, Guang Jun Liu , 2011, Advanced Materials Research ,Volume 413, Pg: 371-374,2011
25. Claudia Malerba, Francesco Biccari, Cristy Leonor Azanza Ricardo, Mirco D’Incau, Paolo Scardi, Alberto Mittiga, 2011, solar energy materials & Solar cells,Volume: 95, Pg: 2848–2854

26. K.R. Balasubramaniam, V.M. Kao, J. Ravichandran, P.B. Rossen, W.Siemons, J.W. Ager, 2012,thin solid films,Volume 520, Pg:3914–3917.
27. Ramaiah K. S. 2001. Material Chemistry and Physics, volume: 22 Pg: 68
28. Chandra S., Pandey R. K. and Agrawal R. C ,1980. Jour. Phys. D. Appl. Phys, volume: 13, Pg: 9
29. Osuji R. U. 2003,Nig. J.of Solar Energy, volume: 14, Pg: 90
30. R.A. Chickwenze and M.N. Nnabuchi, 2010 , Chalcogenide Letters, volume:7,Pg: 389-396
31. B.R. Sankapal, R.S. Mane, C.D. Lokhande,2000, Materials Chemistry and Physics, volume:63,Pg: 230-234
32. S. R. Yoganaranrasimhan and C. N. Rao, 1996, Trans. Faraday Soc., Volume 58, Pg: 476
33. Ezenwa I. A, Ekpunobi A.J, and Ekwo . P, 2003, Natural and Applied Sciences Journal, volume: 11, Pg: 193-196
34. M.Mahaboob Beevi , M.Anusuya, V.Saravanan,2010, International Journal of Chemical Engineering and Applications, volume: 1,Pg:2-5
35. Rodrigo Cue S, S.Velumani, P.J.Sebastian and J.A.Chavez-Carvayar, 2010,Journal of New Materials for Electrochemical Systems, volume:13 Pg:7-14.
36. Mohd Rafie Johan, Mohd Shahadan Mohd Suan, Nor Liza Hawari ,Hee Ay Ching,2011, Int. J. Electrochem. Sci.,volume: 6 Pg: 6094 - 6104
37. Ikhmayies S.J. and R.N. Ahmad-Bitar, 2010, J. of Appl. Sci. volume: 9, Pg: 1141